



**Politecnico
di Torino**

Politecnico di Torino

Master Thesis Report

Master's Degree

September 2022

Consensus-Based Approach for the Primary and Secondary Controls of Microgrids

Supervisors:

Serge Pierfederici (Professor, Université de Lorraine)

Massimo Santarelli (Professor, Politecnico di Torino)

Author:

Rida Sohail



Abstract

The development of electric transportation systems and the massive integration of renewable energy sources into the electrical grid contribute to the development of microgrids for both stationary and embedded applications. Thus, it is of utmost importance to formulate the energy/power management strategies for such microgrids.

In this project, an AC microgrid is considered comprising of different Distributed Generation sources (DGs), in Grid forming operating mode, connected in Mesh topology. The consensus approach based on Graph theory is used to achieve accurate active and reactive power sharing between DGs (Primary control) as well as system parameters' restoration after disturbance in the overall system (Secondary control). Special attention has been paid to deal with the communication delays between DGs which affect the stability of the system. Moreover, control parameters are designed, and their effect is taken into account on the stability and dynamics of the system.

Acknowledgments

I would like to first thank Serge Pierfederici, Professor at Université de Lorraine, for providing me with this opportunity to work on the most recent and challenging problem in microgrids. It was an honor for me to work under his supervision where I get a chance to witness his immense and profound knowledge in the domain of power electronics. His incredible guidance throughout the project not only facilitated me in strengthening my concepts but also enhanced my vision of finding the solutions to the technical problems myself. Despite his tough schedule, he always welcomed me and tried to clear my concepts and difficulties which I faced in this project.

I would also like to thank Youssef Hennane, a Post-doctoral student at LEMTA, who provided immense support throughout my master thesis. Through his guidance, I was able to grasp the background of the project very quickly. I would like to thank him for always steering me in the right direction whenever required.

Also, I would like to thank my academic supervisor, Massimo Santarelli, Professor at Politecnico di Torino. I truly appreciate that despite his busy routine which includes mobility for various conferences across the world, he always made me aware of his availability.

In addition, I would like to express my sincerest gratitude to the Management of Erasmus Mundus program Decentralized Smart Energy Systems (DENSYS) for giving me this opportunity to study at two renowned universities in France and Italy and to work on real-life challenging problems to tackle climate change and global warming. I would like to specially mention Fabrice Lemoine, Chair of the DENSYS program, for his extensive support and cooperation throughout these 2 years. I would also like to thank my colleagues who accompanied me on this exciting journey of 2 years in DENSYS.

Last but not the least, the most important people in my life; my parents, my siblings, my husband, and my little princess (my daughter). I truly believe that I could not have made it this far without the efforts of my father, without the never-ending prayers of my mother, without the strong support of my sister, and without the faith, my husband had in me who trusted in my abilities and allowed me to pursue my dream of completing this graduate program in Europe.

Rida Sohail

29-August-2022

Table of Contents

Abstractii

Acknowledgmentsiii

Nomenclature.....vi

Laboratoire Énergies & Mécanique Théorique et Appliquée (LEMTA)vii

Chapter 1 - Introduction..... 1

 1.1. Background..... 1

 1.2. Scope of Work and Research Objectives..... 3

Chapter 2 - Literature Review 4

 2.1 Types of Microgrids 4

 2.2 Control of Distributed Generators (DGs)..... 5

 2.2.1. Grid-Forming Converters..... 5

 2.2.2. Grid-Following Converters..... 6

 2.3. Hierarchical Control Structure in Microgrids 7

 2.3.1. Primary Control 7

 2.3.2. Secondary control..... 10

 2.3.3. Tertiary control..... 10

 2.4. Control Approaches..... 11

 2.4.1. Centralized Control..... 11

 2.4.2. Decentralized Control..... 11

 2.4.3. Distributed Control..... 12

 2.5. Graph Theory..... 12

 2.6. Consensus in Linear Multi-Agent Systems (MAS)..... 15

Chapter 3 - Control of AC Mesh Microgrid..... 16

 3.1. Development of Primary Control Strategies – Centralized Approach..... 16

 3.1.1. Droop Control for Active and Reactive Power Sharing in Islanded Mesh Microgrids..... 17

 3.1.2. Modified Droop Control for Accurate Reactive Power Sharing in Islanded Mesh Microgrid
18

 3.2. Development of Distributed Primary Control Strategy - Using Consensus Theory..... 22

 3.2.1. Modified Droop Control for Accurate Reactive Power Sharing 22

 3.3. Development of Distributed Secondary Control Strategies – Using Consensus 27

 3.3.1. Restoration of DGs Frequency to Rated Frequency 27

 3.3.2. Restoration of DGs Voltage Close to Rated Voltage..... 31

Conclusion 37

References..... 38

Nomenclature

- AC** - Alternating Current
- DC** - Direct Current
- DER** - Distributed Energy Resource
- DG** - Distributed Generator
- ESS** - Energy Storage System
- MAS** - Multi-Agent System
- MG** - Microgrid
- PCC** - Point of common coupling
- SOC** - State of Charge
- VCM** - Voltage Control Mode
- VSI** - Voltage-Source Inverter

Laboratoire Énergies & Mécanique Théorique et Appliquée (LEMTA)

Laboratoire Énergies & Mécanique Théorique et Appliquée (LEMTA) is the joint research unit of Université de Lorraine and the Centre National de la Recherche Scientifique (CNRS). It is further organized into three diverse and different research groups which mainly deal with and produce novel research outcomes in the field of Mechanics, Energy, and Processes.

It has been almost 50 years since LEMTA came into existence and gained experience in the field of Mechanics and Transfers. In the past few years, global warming and climate change have been alarming issues, so LEMTA has aligned its research objectives toward the Energy transition. To overcome the major challenges and obstacles in Industrial growth, and in the domain of energy, LEMTA always put efforts into providing a feasible and economical solution by utilizing its extensive research experience in the fields of Fluid mechanics, thermal engineering, electrochemical systems, and electrical systems.

Chapter 1 - Introduction

1.1. Background

In the conventional power system, power flows unidirectionally from generation sources to the load via transmission and distribution networks. However, in the past few years considerable focus has been made on the research and development of new technologies associated with power systems because of the environmental issues raised by the burning of fossil fuels, the alarming situation of global warming as well as the due to the problems caused by the penetration of massive intermitted renewable energy sources [1].

With the development and advancement of Distributed Energy Resources (DERs) such as photovoltaic panels, wind turbines, fuel cells, electrolyzers, battery storage systems, etc., Microgrids (MGs) have gained massive attraction and attention as DERs can be easily integrated into power system with the help of them [1]. There are two modes of operation of MGs: islanded mode and grid-connected mode.

The fundamental elements that form a MG are described as follows [2]:

- **Distributed Generator (DG):** DGs are the sources integrated into the MGs to supply energy to the connected load. They can either be operated as current or power sources or as voltage sources. Their operation as voltage source establishes the voltage and frequency in the MG. Photovoltaic panels, and wind turbines are examples of DGs that act as sources.
- **Energy Storage System (ESS):** To overcome the intermittent nature of renewable energy sources and to increase the reliability as well as power quality of the network, energy storage systems are integrated into the MGs. In addition, ESS is also capable of enhancing the overall performance of MGs.
- **Loads:** MGs supply energy to the different kinds of loads connected to them such as residential or industrial. The loads can be further classified as critical or non-critical loads.

Besides the elements mentioned above, MGs require other infrastructures:

- **Point of common coupling (PCC):** As discussed above, MGs operate in grid-connected mode, and in that case, PCC serves as a gateway between MG and the main grid. Different equipment can form this connection such as switchgear, circuit breakers or power converters. MG can be mono-PCC as seen in Figure 1.1 or DGs forming MG can be connected in a mesh topology forming multi-PCC mesh MG which is shown in Figure 1.2.
- **Distribution lines:** DERs and loads are connected through distribution lines which could be single phase or three phases.
- **Power converters:** Many DERs produce DC energy [3] and thus cannot be directly connected with the AC system or MG. So, the power converter (DC/AC or AC/DC/AC) is required. Different types of power converters are used depending on the operation modes of the MG.

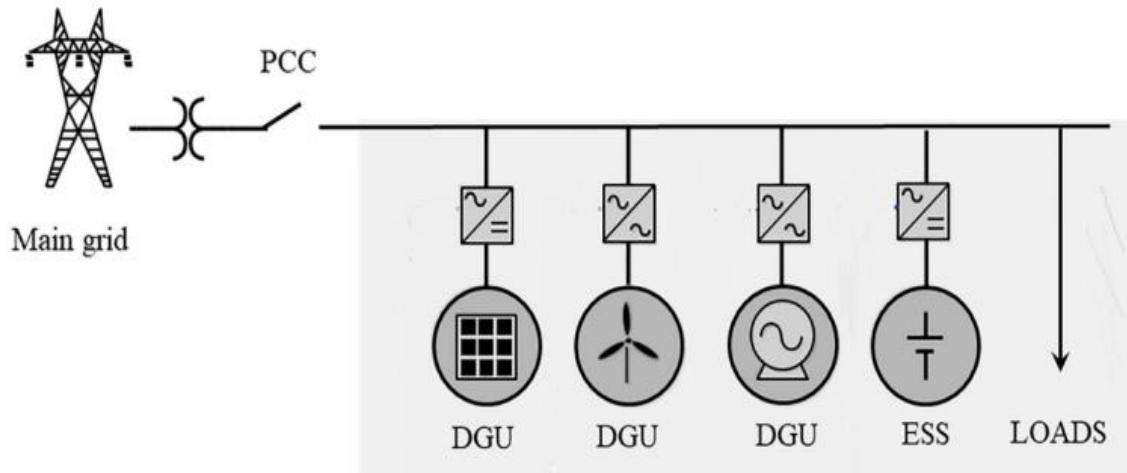


Figure 1.1 - Microgrid with one point of common coupling (PCC) [4]

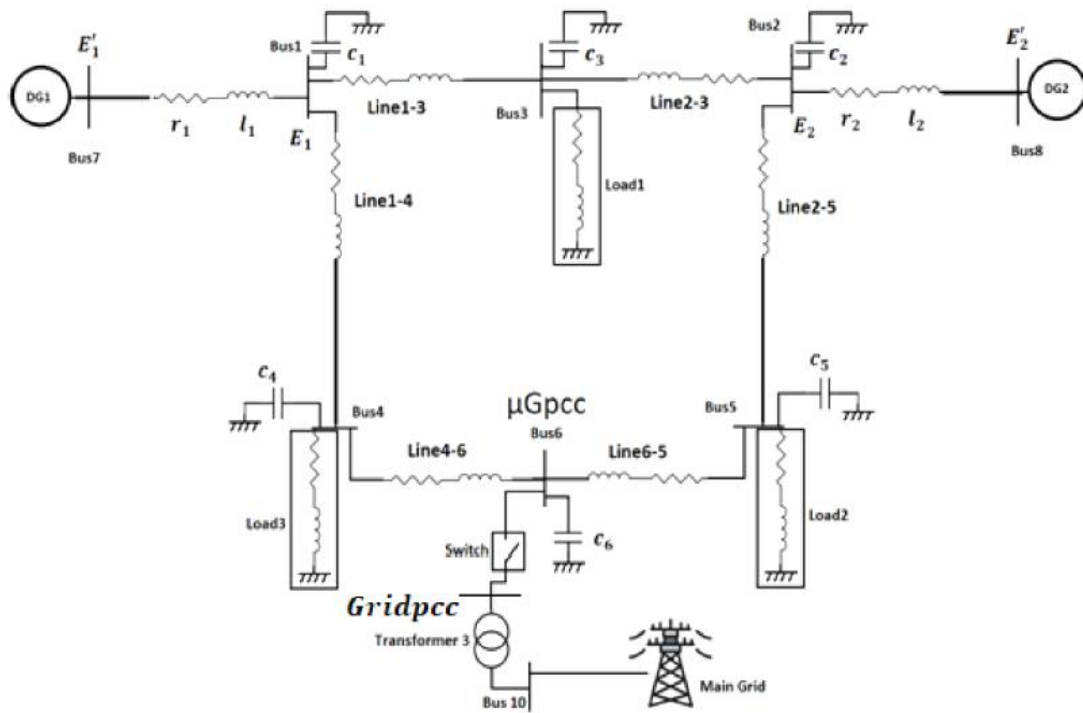


Figure 1.2 - Multi-PCC Mesh- Type MG inspired from IEEE 9 bus system [5]

1.2. Scope of Work and Research Objectives

In the last few years, the penetration of renewable energy sources into microgrids made them more vulnerable to the risks of instability. However, the use of controllable power converters reduces these risks as they allow a fast and dynamic response to sudden load variations. Among different topologies of Microgrids, Mesh-type microgrids are better as compared to microgrids with a single point of common coupling (PCC) in terms of power availability. As we know that microgrids can be operated in islanded mode, but the intermittent nature of renewable energy sources cannot allow the operation of a microgrid in the islanded mode for a long time. Therefore, microgrids should be capable of operating in the grid-connected mode for reliable operation. In islanded as well as grid-connected microgrid operating modes, the load power should be shared equally by the DG units in proportion to their power ratings [6], so that the aging and stress on the sources could be avoided. The active power-frequency ($P-\omega$) and reactive power-voltage ($Q-V$) droop control method is the most commonly used approach to achieve accurate power sharing in MGs [6]. However, due to impedances of power lines in the MGs, there is a voltage drop which results in the power coupling phenomena that ultimately results in inaccurate reactive power sharing [7], [8]

To address the problem of inaccurate reactive power sharing in MGs, the authors of [5] proposed a modified droop control strategy. The non-linear control strategy which modifies the conventional droop control has resulted in accurate active and reactive power sharing between DGs integrated into the MG. However, that non-linear control is based on a centralized approach where information of the reference potential needs to be communicated to all DGs in the network to achieve accurate reactive power sharing. There are many disadvantages associated with the centralized approach, communication failure being one of them, which are discussed in detail in the Literature review section.

To avoid the disadvantages associated with the centralized approach, distributed control is adopted and applied to the modified droop based on the non-linear control. The research objectives of this project are to:

- Investigate modified droop control methods for accurate power sharing between DGs in islanded mesh microgrids as proposed by authors in [5]
- Propose a fully Distributed Primary control strategy based on Droop control for DGs active and reactive power sharing in islanded mesh microgrids.
- Propose a fully Distributed Secondary control strategy for voltage and frequency restoration to the rated values.
- Propose a robust design for the primary and secondary control parameters.
- Prove the efficiency of the proposed strategies by simulations using the Simscape toolbox of MATLAB/Simulink.
- Study the robustness of the proposed control concerning load variation and topology changes.

Chapter 2 - Literature Review

2.1 Types of Microgrids

MGs can be classified into three different types based on the output voltage fed to the load [9].

- DC MG
- AC MG
- AC/DC hybrid MG

As can be seen in Figure 2.1, in an AC MG, there is a common AC bus to which all DGs and ESS are connected with the help of power converters [9]. All DGs such as PV panels, wind turbines, and other storage systems produce DC so converters are required to connect them with the AC power line.

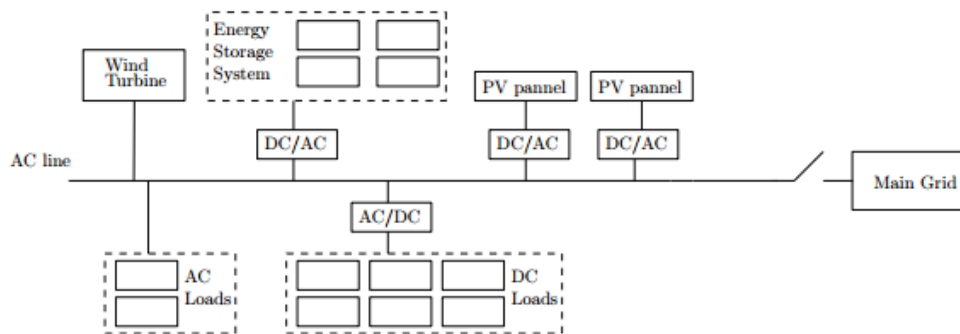


Figure 2.1 - Structure of an AC-MG with a single power line [9]

Whereas in DC MGs, there is a common DC bus to which all the DGs and storage units are connected as can be viewed in Figure 2.2. This is the most common type of MG in recent times as the majority of the renewable energy sources and storage systems produce DC. They possess a wide range of applicability, higher efficiency, and are simple in their operation due to which they have increased great attention in recent times [9], [10].

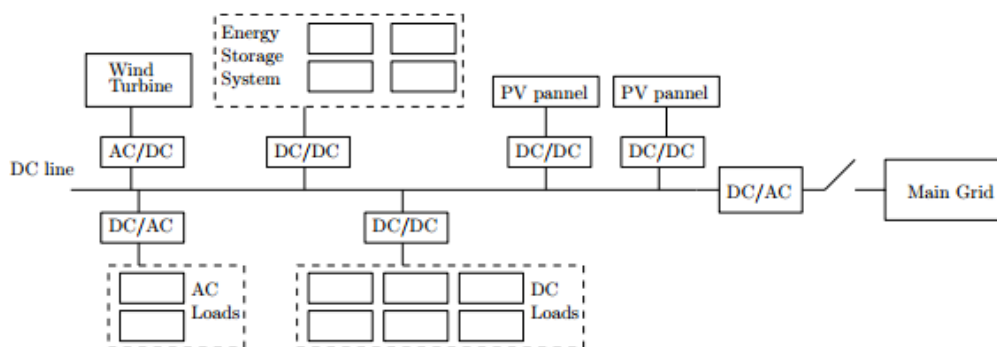


Figure 2.2 - Structure of a DC-MG with a single power line [9]

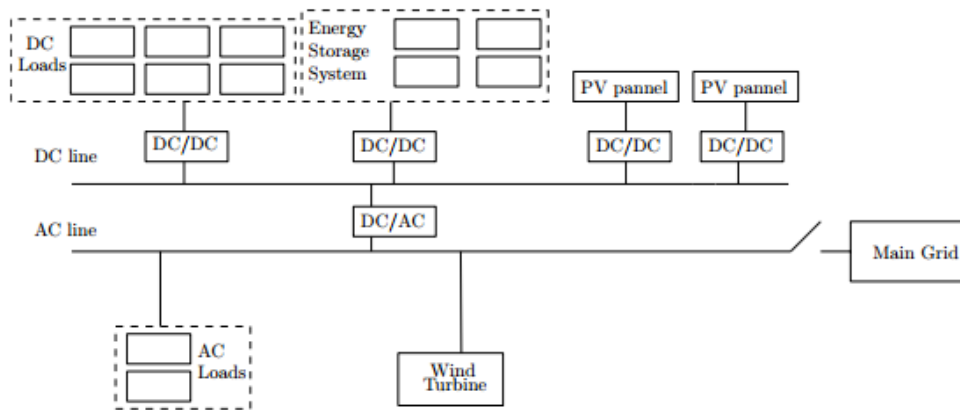


Figure 2.3 - Structure of an AC/DC hybrid MG [9]

However, in hybrid AC/DC MGs, as the name suggests, both types of buses AC as well as DC are present in the system. Different power converters are used to interconnect different DERs, and ESS with the power lines as can be seen in Figure 2.3 [9].

2.2 Control of Distributed Generators (DGs)

The power converters can be of various types depending on the output produced by DERs and the type of bus (AC/DC) to which the components in MGs are connected. The types include DC/DC, AC/AC, DC/AC, AC/DC, or AC/DC/AC. When the DERs and ESS such as PV, hydrogen storage, and battery storage are used which produce DC, then DC/DC or DC/AC converters are used significantly. Whereas sources that produce AC use AC/DC, AC/AC, or AC/DC/AC type of power converters. These power converters can be classified as grid-forming or grid-supporting converters depending on their mode of operation [11], [12].

2.2.1. Grid-Forming Converters

In the absence of main grid voltage, MG operates in islanded mode, and to set the voltage in the MG system, the power converters operate in grid-forming mode. The grid-forming converter, therefore, behaves as an ideal voltage source having low impedance at the output, and is thus said to be operating in voltage control mode (VCM) [13]. In DC MG, VCM includes the control of voltage magnitude but for AC MG, it included both control of voltage magnitude as well as frequency. In an islanded AC MG comprising multiple converters, there should be at least one converter that should operate in grid-forming mode to set the frequency and voltage in the network. In the case of more than one converter operating in grid-forming mode, all of them need to be synchronized with each other [14], [15]. There exist different synchronization strategies such as droop control, external synchronization signal used in PLL of inverters, etc.

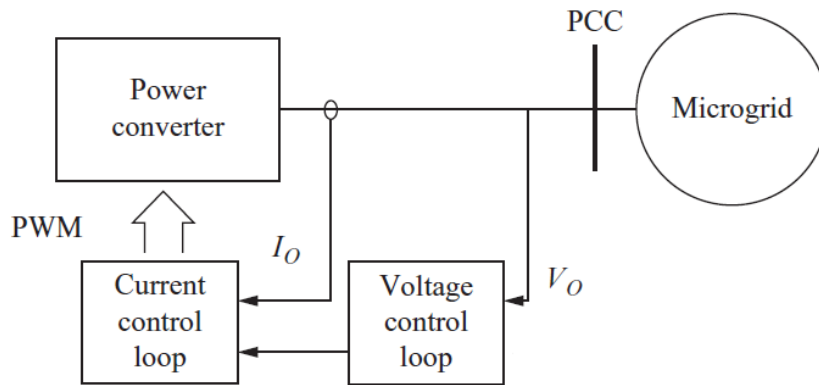


Figure 2.4 - System and control diagram for Grid-Forming power converter [11]

The power converter operating in grid-forming mode can be observed in Figure 2.4. The PCC voltage is set by the grid-forming converter and to control this voltage, the two-loop control scheme has been implemented which consists of an outer voltage loop and an inner current loop. Where the reference for the inner current control loop is generated by the outer voltage control loop [11].

2.2.2. Grid-Following Converters

The grid-following converters unlike grid-forming converters just follow the frequency and voltage imposed by the main grid in the network. They act as a current source and transfer active and reactive power to the grid as per the power or current setpoint. These are the most common type of converters used today in various applications. In these types of power converters, the control structure should first synchronize with the grid using the phase-locked loop (PLL) technique. The overall control structure remains the same as a grid-forming converter comprising of an outer voltage control loop and an inner current control loop [12] [16].

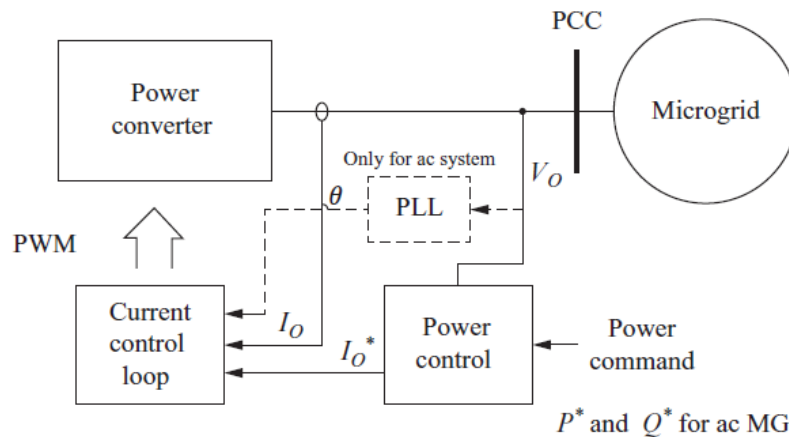


Figure 2.5 - System and control diagram for Grid-Following power converter [11]

The control system of the grid-following converter can be seen in Figure 2.5. To regulate the power fed by the converter, the converter output current is taken as the feedback. From the reference real and reactive power P^* and Q^* in the power control loop, a reference current has been generated [11].

2.3. Hierarchical Control Structure in Microgrids

Proper control of MG is a requirement for stable and economically efficient operation. The principal roles of the MG control structure are [1].

- Voltage and frequency regulation for both operating modes (Islanded and grid-connected).
- Proper load sharing and DER coordination.
- MG resynchronization with the main grid
- Power flow control between the MG and the main grid.
- Optimizing the MG operating cost.
- Providing ancillary service.

These requirements are of different significances, timescales, and infrastructure investment, thus requiring a hierarchical control structure to address each element at a different control hierarchy [1].

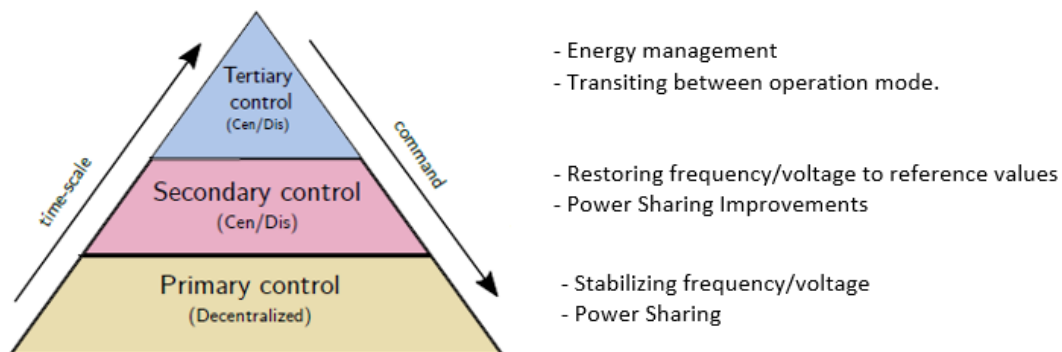


Figure 2.6 - The hierarchical control structure of MGs

Figure 2.6 shows a hierarchical structure comprised of primary, secondary, and tertiary control that is used to control MG.

2.3.1. Primary Control

The primary control is typically based on droop control. It features the fastest response being at the first level in the control hierarchy. This type of control does not require any communication and is based on local measurements [17].

The primary control satisfies the following requirements [1].

- To stabilize the voltage and frequency: When an islanding event or variation of generation or load event happens, the MG may lose its voltage and frequency stability due to the mismatch between the power generated and consumed.
- To properly share the active and reactive power among DGs.
- The primary control should have the fastest response to any variation (about 100 milliseconds in grid forming mode), which can be assisted to improve power reliability.

In literature, various strategies at the primary control level can be found which are classified based on communication requirements. Communication-based controllers include master/slave control and

central control. Controllers without communication are generally based on the droop concept [1]. Figure 2.7 lists the primary control strategies in islanded MGs.

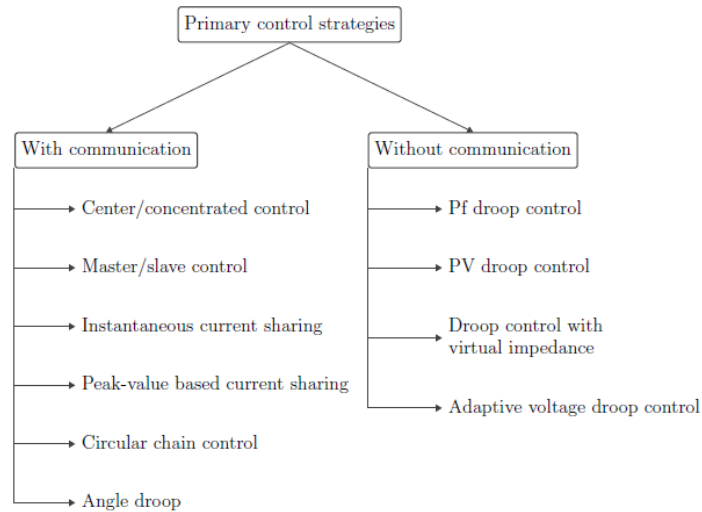


Figure 2.7 - Primary Control Strategies in MGs

Voltage-Source Inverters (VSIs) used as an interface for DC sources in MGs, or as part of back-to-back converters, require a specially designed control to simulate the inertia characteristic of synchronous generators and provide appropriate frequency regulation. For this purpose, VSI controllers are composed of two stages [17]:

- **Inverter output controller:** It controls and regulates the output voltages and current of DGs in MG. [18]–[22]. It typically consists of an outer loop for voltage control and an inner loop for current regulation. PI controllers are commonly used to design both control loops.
- **DG power-sharing controller:** This type of controller is responsible for the adequate share of active and reactive power mismatches in the microgrid [18]–[22]. To perform power sharing, active power-frequency and reactive power-voltage droop controllers are used which do not require any sort of communication and emulate the droop characteristics of a synchronous generator [23].

2.3.1.1. Droop Control

In grid supporting power converters, to control the exchange of active and reactive power with the network and to keep the grid voltage magnitude and frequency under control, droop control is implemented. Droop characteristics represent the self-regulation capability of the synchronous generator in grid-connected mode. When the frequency increases, the active power will be decreased and when the voltage magnitude increases, the injected reactive power is decreased [1].

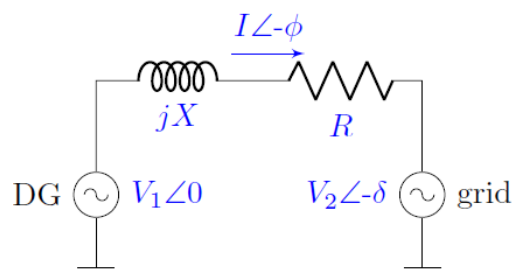


Figure 2.8 - Simplified power flow diagram between DG source and the grid [1].

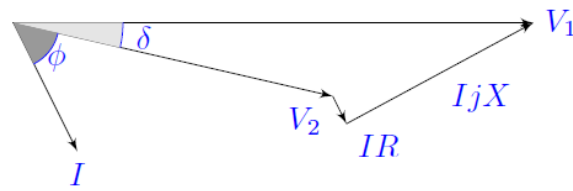


Figure 2.9 - Vector diagram [1]

In Figure 2.8, it can be seen that the power converter as an ideal controllable voltage source is connected to the grid through line impedance. The active and reactive powers that will deliver to the grid can be written as follows based on the vector diagram shown in Figure 2.9.

$$P_1 = \frac{V_1}{R^2 + X^2} [R(V_1 - V_2 \cos \delta) + XV_2 \sin \delta] \quad 2.1$$

$$Q_1 = \frac{V_1}{R^2 + X^2} [-RV_2 \sin \delta + X(V_1 - V_2 \cos \delta)] \quad 2.2$$

where P_1 and Q_1 are the active and reactive powers, respectively, flowing from the 1 (power converter) to the main grid 2, V_1 and V_2 are the voltage magnitudes, δ is the phase-angle difference between the two voltages, $Z = R + jX$ is the line impedance and Φ is the impedance angle [1].

Assume that the inductive component of the line impedance is much higher than the resistive component. The power angle δ in such lines is small, so it can be assumed that $\sin \delta \approx \delta$, $\cos \delta \approx 1$. The equations can be rewritten:

$$\delta = \frac{XP_1}{V_1 V_2} \quad 2.3$$

$$V_1 - V_2 = \frac{XQ_1}{V_1}$$

The above equations show a direct relationship between the power angle δ and the active power P , as well as between the voltage difference ($V_1 - V_2$) and the reactive power Q . These relationships permit regulating the grid frequency and voltage at the point of connection of the power converter, by controlling the value of the active and reactive powers delivered to the grid. Therefore, the following droop control expressions can be written [1]:

$$f - f^{ref} = -k_p (P - P^{ref}) \quad 2.4$$

$$V - V^{ref} = -k_Q (Q - Q^{ref})$$

where $f - f^{ref}$ and $V - V^{ref}$ represent the grid frequency and the voltage deviations respectively, and $(P - P^{ref})$ and $(Q - Q^{ref})$ are the variations in the active and reactive powers delivered by the power converter to compensate for such deviations [1].

The relationships between P and f , V and Q can be represented graphically as shown in Figure 2.10. The k_p and k_Q parameters set the slope of the frequency and voltage droop characteristics [1].

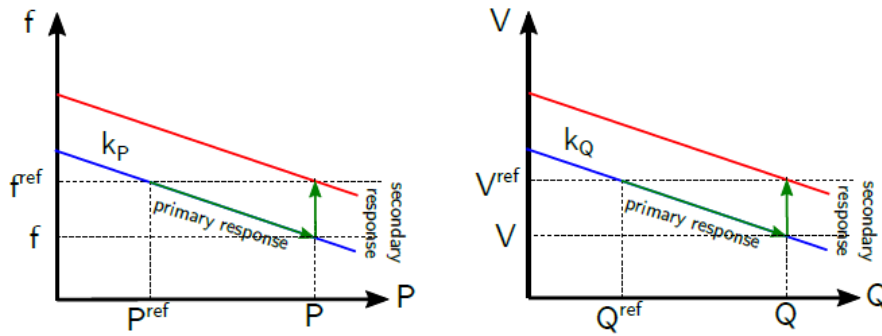


Figure 2.10 - Frequency and voltage droop [1]

The conventional droop method can be implemented without communication links, and therefore, is more reliable. However, it has some drawbacks as listed below [24]:

- The conventional droop method is developed assuming highly inductive effective impedance between the DGs and the AC bus. However, this assumption is challenged in MG applications with low-voltage levels.
- As opposed to the frequency, the voltage is not a global quantity in the MG. Thus, reactive power control may adversely affect voltage regulation.

2.3.2. Secondary control

The secondary control, with communication requirements in slower dynamic response, is designed to achieve objectives that resolve the drawbacks of primary controllers.

- **Frequency and Voltage restoration:** Primary control may cause frequency deviation even in the steady state. The secondary control restores the MG voltage and frequency and compensates for the differences. The frequency of the MG and the bus voltage of a given DG are compared with the corresponding reference values, ω^{ref} and V^{ref} . Then, the error signals are processed by individual controllers, and the results ($\delta\omega$ and δV) are sent to the DG controller to compensate for the frequency and voltage deviations.

2.3.3. Tertiary control

The tertiary control level takes charge of optimizing the MG operation and setting its interaction with the distribution network by controlling the active and reactive power references for each DG unit [1].

In the islanded mode, this control level considers the economic and technical concerns in the optimal operation or deals with the optimal power flow problem within the MG [1].

In the grid-connected mode, the common objectives of tertiary control are to minimize the price of energy import at the PCC, improve the power factor at the PCC, and optimize the voltage profile within the MG [25], [26].

The power flow, within MGs or between MGs and the main grid, can be managed by adjusting the reference voltage amplitude and frequency of DGs. First, active and reactive output powers of the DGs, P , and Q , are measured. These quantities are then compared with the corresponding reference values P^{ref} and Q^{ref} to obtain the frequency and voltage references ω^{ref} and V^{ref} based on:

$$\omega^{ref} = k_{pp}(P^{ref} - P) + k_{IP} \int (P^{ref} - P) \quad 2.5$$

$$V^{ref} = k_{PQ}(Q^{ref} - Q) + k_{IQ} \int (Q^{ref} - Q)$$

where k_{PP} , k_{IP} , k_{PQ} and k_{IQ} are the controllers' parameters. ω^{ref} and V^{ref} are used as reference values to the secondary control [1].

2.4. Control Approaches

Regarding the implementation of each control layer (shown in Figure 2.6), for any of the MG topologies such as AC-MG, DC-MG, and hybrid MG, three implementation methodologies could be applied. These are based on centralized, distributed, and decentralized topologies as can be seen in Figure 2.11. A brief discussion of each implementation methodology is shown below[27]:

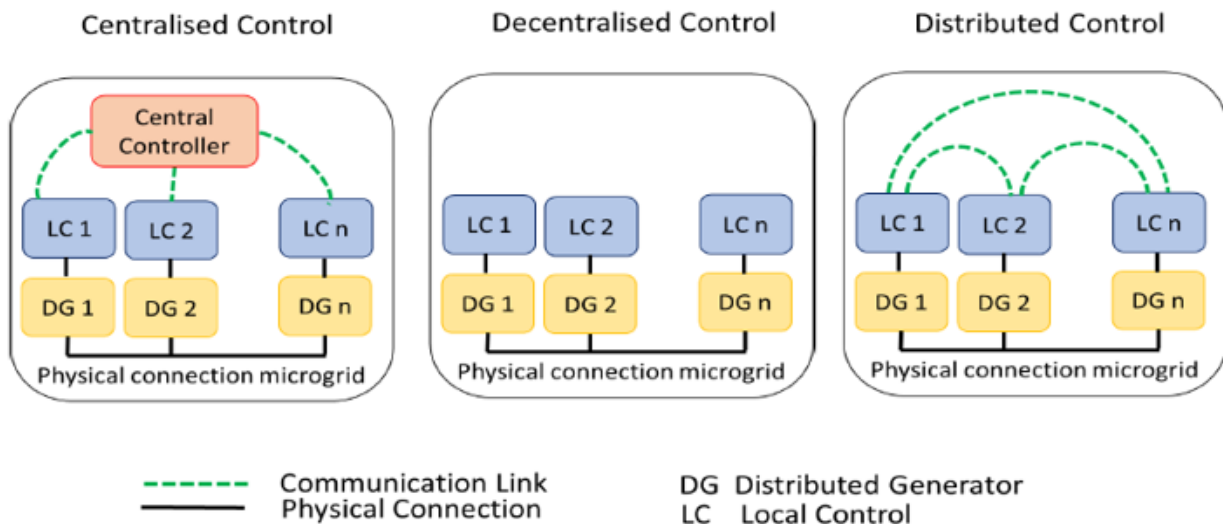


Figure 2.11- Classification of MG topologies according to the communication networks utilized for control purposes [28]

2.4.1. Centralized Control

The centralized architecture can be viewed in Figure 2.11 (a). There is a central controller that gathers all the information from all the local controllers, performs the calculations, and in the end, sends back the commands to each local controller. The central unit is responsible for bulk computations and decision-making. Centralized control is common in traditional power systems, but they are no longer suitable for the larger number of DERs due to the following main reasons [29]–[32]:

- reliability and security susceptibility of the central controller as a common point of failure.
- communication requirements due to the geographical span.
- reluctance to share data of participant actors.
- excessive computation in the central unit due to numerous controllable loads and generators.

Centralized techniques although they own several advantages such as the system need only a central controller, require more simple technique due to the gathering of data into one single unit, the convergence in solution is more guaranteed, etc.; they, with the above drawbacks, are most probably not the best choice better solutions for providing the required functionality for operating microgrids.

2.4.2. Decentralized Control

In this case, the control system of each DER unit (agent) is implemented utilizing local measurements only which can be seen in Figure 2.11 (c). The control methodologies are usually based on V-Q and f-

P droops [28], [33], [34]. By using droop controllers, the MG load is shared between the DG units according to their power capabilities through a physical link [28]. Notice that this methodology lacks communication channels and this certainly makes challenging to implement secondary and tertiary control systems [27].

2.4.3. Distributed Control

In distributed control, the central controller is not necessary as can be seen in Figure 2.11 (b) because the control effort is distributed along with the MG, with 'agents' operating in a supportive way to obtain global objectives [35]–[37]. The main advantages of the distributed approach are as follows [1]:

- The system failure in MGs is easily avoidable because the central controller which controls the overall system is neglected.
- As only limited information is exchanged among adjacent agents, so the communication bandwidth can be reduced to a greater extent.
- the distributed framework is more flexible and adaptive concerning the changes of systems, especially in view that the topology of the electricity grid and the communication infrastructure in the smart grid are likely to be more dynamic.
- the system is easily extendable (plug and play), if a new load or DG is added, it can immediately start communicating with the adjacent units and the system as a whole can automatically reach a stable operating condition.

Some drawbacks of the distributed scheme have also been pointed out as follows[38], [39]

- The first is the more demanding on the ICT infrastructure, meaning that more messages and data have to flow between the nodes of the network, instead of only communication flows between central and local units. However, this is correct only for a centralized system, where the central unit fails to find a solution if the communication with one of the nodes fails. In the case of a distributed approach, the solution could be found despite some failures of communication lines.
- The second is the trade-off in speed when solving a control problem. The solution of local control signals may require some iterations for computation and communication exchange. However, in the hierarchical control, the high control level, where the distributed computation takes place, does not need a fast response but at a slower time scale. Therefore, distributed algorithms still can be applied for control and optimization in MGs.

Overall, the distributed strategy has outstanding advantages over the traditional centralized strategy. The distributed approach is considered the promised alternative solution for the control and management of the next generation of power systems, especially in MGs with the increasing integration of controllable entities [1].

2.5. Graph Theory

Usually, graph theory is used to describe the structural properties (topology) of a network. It gives an abstraction of how the information is exchanged between agents in a network [9]. This high-level description is done in terms of objects referred to as vertices and edges. In this section, we recall some definitions and properties from [40], [41]

A finite graph G is composed of a finite set of elements that we call the vertex set and denote by V . The vertices represent the elements of the graph; the set V can be represented as [9]:

$$V = \{1, 2, 3, \dots, n\}$$

The interconnection between the vertices is described by a subset of $V \times V$ called the edges set; denoted by \mathcal{E} .

There are some most terms in Graph Theory that are defined as follows [9]:

- **Neighborhood:** The neighborhood $N_i \subseteq V$ of the vertex i is defined by the set $\{j \in V \mid (i, j) \in \mathcal{E}\}$
- **Undirected Graph:** A graph G is undirected if for all $i, j \in V$

$$(i, j) \in \mathcal{E} \Rightarrow (j, i) \in \mathcal{E}$$

Otherwise, the graph is directed.

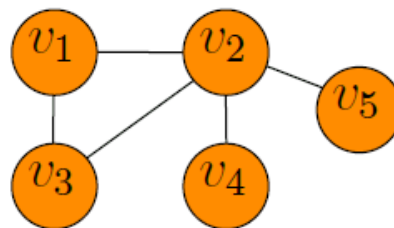


Figure 2.12 - Example of an undirected (Connected) graph with 5 vertices and 5 edges [9]

Figure 2.12 shows an example of a graph where the vertex set is $V = \{1, 2, 3, 4, 5\}$ and the adjacency set is $\mathcal{E} = \{(1,2), (1,3), (2,3), (2,4), (2,5)\}$. Two vertices are neighbors (adjacent) if there is at least one edge between them.

- **Connected Graph:** A graph G is connected if for every pair of vertices there is a sequence of distinct vertices i_0, \dots, i_m that relate it such that for $k = 0, 1, \dots, m - 1$, the vertices i_k and i_{k+1} are adjacent; if not, graph G is disconnected.

For example, the graph in Figure 2.12 is connected and the graph in Figure 2.13 is disconnected.

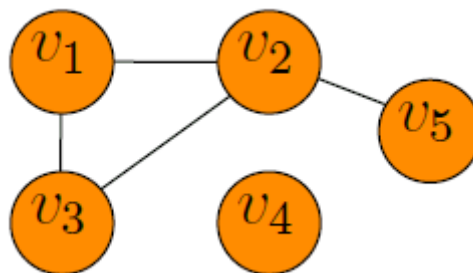


Figure 2.13 -Example of an undirected (Disconnected) graph with 5 vertices and 5 edges [9]

Graphs can be presented not only by graphical representation but also using matrices. For an undirected graph G , the degree of a given vertex $i \in V$ is the cardinality of the neighborhood set N_i , that is, it is equal to the number of vertices that are adjacent to the vertex i . Thus, for the graph in Figure 2.12, the degrees of the vertices are:

$$d(1) = 2, d(2) = 4, d(3) = 2, d(4) = 1, d(5) = 1$$

- **Degree Matrix:** The degree matrix $D \in \mathbb{R}^{n \times n}$ of a graph G with n vertices, is the diagonal matrix, containing the vertex-degrees of G on the diagonal, that is,

$$D = \begin{bmatrix} d(1) & 0 & \dots & 0 \\ 0 & d(2) & \dots & 0 \\ \vdots & \vdots & \ddots & \vdots \\ 0 & 0 & \dots & d(n) \end{bmatrix} \quad 2.6$$

For example, the degree matrix of the graph in Figure 2.12 is

$$D = \begin{bmatrix} 2 & 0 & 0 & 0 & 0 \\ 0 & 4 & 0 & 0 & 0 \\ 0 & 0 & 2 & 0 & 0 \\ 0 & 0 & 0 & 1 & 0 \\ 0 & 0 & 0 & 0 & 1 \end{bmatrix}$$

- **Adjacency Matrix:** The adjacency matrix $A \in \mathbb{R}^{n \times n}$ is the symmetric matrix encoding the adjacency relationship in the graph G , that is,

$$A_{ij} = \begin{cases} 1 & \text{if } (i,j) \in \mathcal{E} \\ 0 & \text{otherwise} \end{cases}$$

The corresponding adjacency matrix of the example shown in Figure 2.12 is:

$$A = \begin{bmatrix} 0 & 1 & 1 & 0 & 0 \\ 1 & 0 & 1 & 1 & 1 \\ 1 & 1 & 0 & 0 & 0 \\ 0 & 1 & 0 & 0 & 0 \\ 0 & 1 & 0 & 0 & 0 \end{bmatrix}$$

- **Graph Laplacian Matrix:** The graph Laplacian matrix is an important matrix representation of a graph which is represented by the equation as follows:

$$\mathcal{L} = D - A$$

The Laplacian matrix of the graph shown in Figure 2.12 is

$$\mathcal{L} = \begin{bmatrix} 2 & -1 & -1 & 0 & 0 \\ -1 & 4 & -1 & -1 & -1 \\ -1 & -1 & 2 & 0 & 0 \\ 0 & -1 & 0 & 1 & 0 \\ 0 & -1 & 0 & 0 & 1 \end{bmatrix}$$

- **Graph:** A graph is a triple $(V, \mathcal{E}, \mathcal{L})$, where $V = \{1, 2, 3, \dots, n\}$ is the node-set, $\mathcal{E} \subseteq V \times V$ is the edge set, and $\mathcal{L} \in \mathbb{R}^{n \times n}$ is the Laplacian matrix.

The following properties will be used in the rest of the thesis [9]:

- If for a given $X \in \mathbb{R}^n$, we have $\mathcal{L}X = 0$, which implies $X = \alpha 1_n$ with $\alpha \in \mathbb{R}$
- There exists an orthonormal matrix $T \in \mathbb{R}^{n \times n}$ that verifies $T^T T = T T^T = I_n$ such that:

$$T^T \mathcal{L} T = \text{diag} (\lambda_1(\mathcal{L}), \lambda_2(\mathcal{L}), \dots, \lambda_n(\mathcal{L}))$$

2.6. Consensus in Linear Multi-Agent Systems (MAS)

A Multi-Agent System (MAS) comprises a set of dynamical systems that are called agents which interact with each other to form a network. MAS is classified into types such as homogenous MAS and heterogenous MAS. In the former type, all agents forming the network can have the same dynamical system whereas, in later types, a dynamical system of agents could be different from each other. The approaches of MAS are inspired by nature such as flocking of birds, a swarm of bacteria, etc. They have several applications in various fields and MGs are one of them [9], [42]

To understand the inter-elemental interactions in MGs, MAS has become an important tool and has gained a lot of attention. DGs and ESS can act as agents which interact with each other through power lines to which they are connected (physical coupling). Since the nature of generation in MGs is distributed so agents (DGs or ESS) partially represent the power network. For instance, an energy storage unit is aware of its state of charge (SOC) and may know the information of the SOC of other energy storage units. But it does not have any idea of what happens in the entire network. Therefore, with the help of coordination between neighboring agents over a certain quantity of interest (consensus), several decisions can be made locally. However, this requires certain rules of communication which specifies that how information is exchanged between the agents which is a consensus algorithm [9].

The most commonly used models to study MAS are decoupled single integrator and double integrator models [43].

Consider a physical linear MAS represented by a connected and undirected graph $G^{phy} = (V^{phy}, \mathcal{E}^{phy}, \mathcal{L}^{phy})$ composed of N linear systems interconnected with the static physical coupling of the form [9]:

$$\begin{aligned} \dot{x}_i &= Ax_i + B_u u_i - B_Z \sum_{j \in N_i^{phy}} \alpha_{ij} (z_i - z_j) \\ z_i &= Mx_i \end{aligned} \quad 2.7$$

With $x_i \in \mathbb{R}^n$, $u \in \mathbb{R}^m$, $z_i \in \mathbb{R}^q$, $\alpha_{ij} \in \mathbb{R}$ and A, B_u, B_Z, M are matrices of appropriate dimensions and N_i^{phy} is the set of neighbors of the agent i concerning G^{phy} . The term $B_Z \sum_{j \in N_i^{phy}} \alpha_{ij} (z_i - z_j)$ represents the physical coupling between the agents [9].

Let us consider that there exist certain output variables of interest for which the agents want to reach an agreement. These variables can be defined as follows [9]:

$$y_i = Cx_i, \quad i \in V \quad 2.8$$

for simplicity we consider y_i as scalar i.e. $y_i \in \mathbb{R}$ and $C \in \mathbb{R}^{1 \times n}$

Chapter 3 - Control of AC Mesh Microgrid

3.1. Development of Primary Control Strategies – Centralized Approach

The Mesh-type AC microgrid considered for this project is inspired by the IEEE 9 bus system. The detailed network can be seen in Figure 3.1. The parameters of the network are summarized in

Table 1 and Table 2.

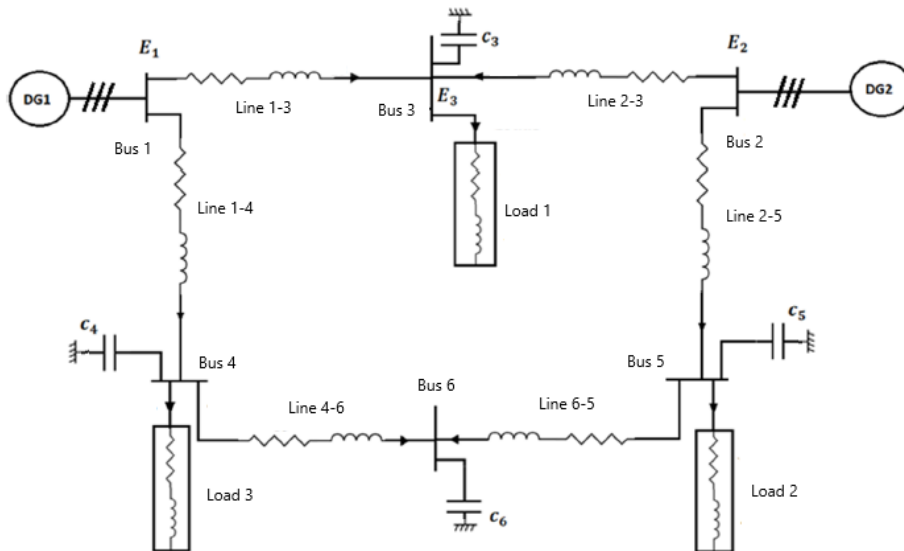


Figure 3.1 - Islanded Mesh AC Microgrid with two DGs

Table 1 - Parameters of the Mesh-type AC microgrid power lines

<i>Lines</i>	<i>Resistance (Ω)</i>	<i>Inductance (mH)</i>	<i>Capacitance (μF)</i>	<i>Points of connections</i>
Line 1-3	0.0629	0.714	20	Bus 1- Bus 3
Line 2-3	0.0629	0.714	20	Bus 2- Bus 3
Line 1-4	0.0629	0.714	20	Bus 1- Bus 4
Line 2-5	0.0629	0.714	20	Bus 2- Bus 5
Line 4-6	0.0629	0.714	20	Bus 4- Bus 6
Line 5-6	0.0629	0.714	20	Bus 5- Bus 6

Table 2 - Sources and loads powers in Mesh-type AC microgrid

<i>Sources/Loads</i>	<i>Rated Active Power (kW)</i>	<i>Rated Reactive Power (kVAr)</i>	<i>Rated Phase to Phase Voltage (V)</i>	<i>Points of connection</i>
Source 1	14.5	5.3	400	Bus 1
Source 2	9.5	3.3	400	Bus 2
Load 1	5	0.7	400	Bus 3
Load 2	4.5	0.9	400	Bus 5
Load 3	4	1	400	Bus 4

3.1.1. Droop Control for Active and Reactive Power Sharing in Islanded Mesh Microgrids

In most practical applications, to achieve accurate active power sharing, the P- ω droop control method is widely used. It also allows frequencies of different DGs integrated into the MG to converge to the same value close to the rated frequency of MG [44], [45]. For the complex topologies of MGs such as Mesh-type AC MGs, the P- ω droop control method remains efficient whereas, Q-V droop control method which imposes the voltages of the DGs in MGs cannot ensure accurate reactive power sharing because of complex MG topology and the impedances of the power lines. The droop equations for power sharing are given as follows [5]:

$$\omega_i = \omega_n - m_i(P_{fi} - P_{in}) \quad 3.1$$

$$E_i = E_n - n_i(Q_{fi} - Q_{in}) \quad 3.2$$

With:

$$m_i = \frac{\Delta\omega}{P_{in}}$$

$$n_i = \frac{\Delta E}{Q_{in}}$$

Where ω_n and E_n are rated values of pulsation and voltage of the i^{th} DG, P_{in} and Q_{in} are rated values of active and reactive power of i^{th} DG. P_{fi} and Q_{fi} are the measured and filtered values of active and reactive power of i^{th} DG. m_i and n_i are the droop control coefficients which are obtained using the permissible variations of DGs pulsation $\Delta\omega$ and ΔE .

Simulation Results

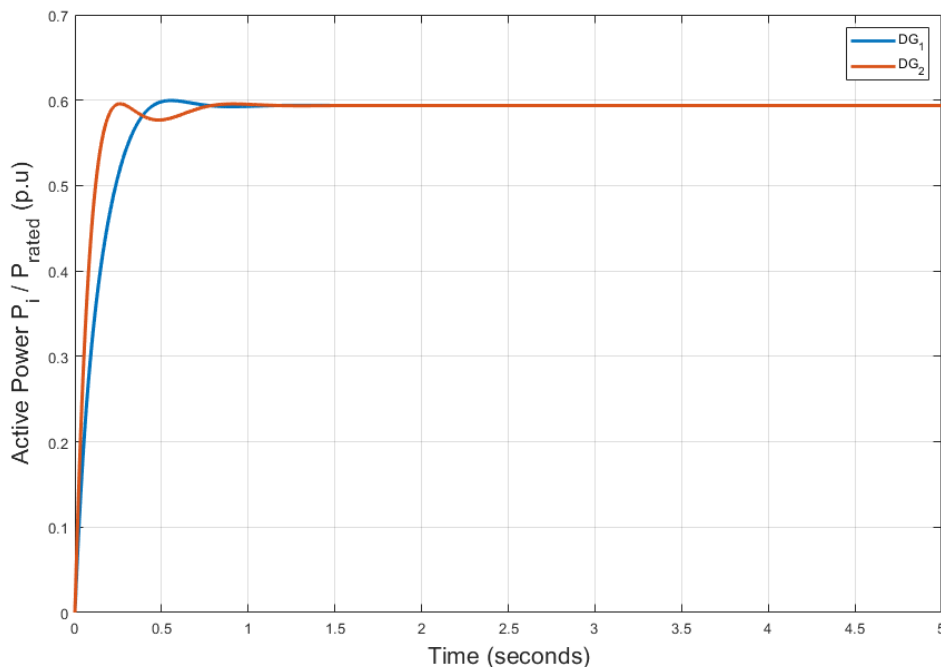


Figure 3.2 - Evolution of active power for both DGs

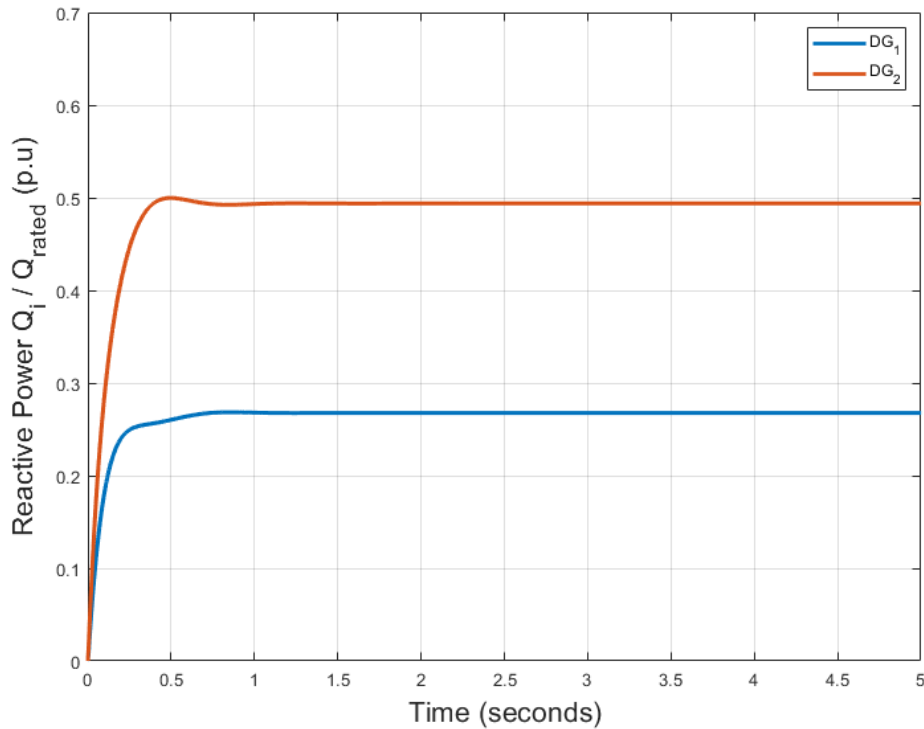


Figure 3.3 - Evolution of reactive power of both DGs

It can be seen in Figure 3.2 that $P - \omega$ droop control applied to a given Mesh-type AC microgrid ensures accurate real power sharing whereas $Q - V$ droop control cannot achieve reactive power sharing between two DGs due to power coupling phenomena and the presence of power lines offering impedance. This requires modification of $Q - V$ droop control which is discussed in detail in the section below.

3.1.2. Modified Droop Control for Accurate Reactive Power Sharing in Islanded Mesh Microgrid

In a mono-PCC microgrid, there is only one common AC bus to which all DGs are connected. The reactive power sharing of such microgrids can be easily improved by comparing the impedance value of the feeders which are connecting DGs to the AC bus. Whereas for mesh-type microgrids, we are dealing with a complex system where it is required to deal with a large number of variables, and thus it is difficult to evaluate system reactive power sharing performance. In mesh-type MGs, each line connecting the PCC_i and PCC_j offers non-negligible inductance $\lambda_{i,j}$ and resistance $\rho_{i,j}$ which results in the voltage drop in the line represented by $\Delta E_{i,j}$ in Eq. 3.3. This voltage drop is proportional to the line current $I_{i,j}$ and is responsible for creating coupling between the active and reactive power $P_{i,j}$ and $Q_{i,j}$ exchanged between PCC_i and PCC_j [5].

$$\Delta E_{i,j} = \rho_{i,j} I_{i,j} \cos \varphi + \lambda_{i,j} \omega I_{i,j} \sin \varphi$$

$$\Delta E_{i,j} = \frac{\rho_{i,j} P_{i,j} + \lambda_{i,j} Q_{i,j}}{E_j} \quad 3.3$$

where E_j is the RMS voltage of the PCC_j

To achieve accurate active and reactive power sharing in complex topologies of MGs such as mesh-type multi-PCC MGs without considering any knowledge of MG structure, the conventional P – ω droop equation expressed in Eq. 3.1 is not modified but Q-V droop control equation as in Eq. 3.2 requires modification by adding to it a non-linear decoupling term expressed in is expressed Eq. 3.5. The modified Q-V droop control equation is expressed in Eq. 3.4. The additional non-linear term $J_i(P_{fi} - P_{in})$ depends on the voltage measured at the pilot node E_{ref} . The power coupling phenomena in complex MGs topologies which is caused by the voltage drop due to inductances and resistances of power lines are removed by the addition of this non-linear term. The value of J_i is estimated by an integral controller which forces error ε_i to zero as expressed in Eq. 3.6. When the ε_i tends to zero in steady state, an accurate reactive power sharing is achieved between different DGs in MGs no what whatever is the power demanded by the load [5].

$$E_i = E_n - n_i(Q_{fi} - Q_{in}) + J_i(P_{fi} - P_{in}) \quad 3.4$$

Where:

$$J_i = K_i \int \varepsilon_i dt \quad 3.5$$

$$\varepsilon_i = \left[-\alpha \left(\frac{E_{ref}}{E_n} - 1 \right) + \left(\frac{Q_{fi}}{Q_{in}} - 1 \right) \right] \quad 3.6$$

To perform the simulations in MATLAB (Simulink), the values of parameters K_i and α are taken from the work of authors [5].

As the mesh-type AC MG considered for this project comprises two DGs shown in Figure 3.1 so each source, DG_1 and DG_2 is modeled by a 3-phase voltage source which is controlled by $E_{abc_{refi}}$ as shown in Figure 3.4 [5]

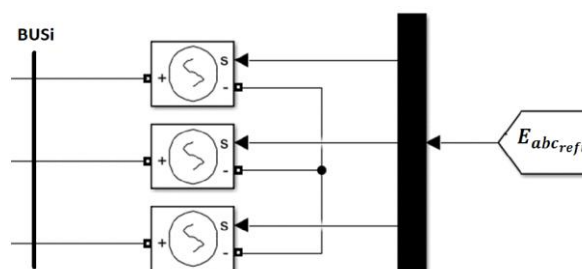


Figure 3.4 - Controllable voltage source which represent DG in mesh-type microgrid [5]

As shown in Figure 3.1, DG_1 and DG_2 are connected to PCC₁ (Bus1) and PCC₂ (Bus 2) respectively. The block diagram describing a droop-controlled DG_i can be seen in Figure 3.5. This block diagram basically shows how to determine $E_{abc_{refi}}$ of the PCC_i to which DG_i is connected. Firstly, voltage and

current vectors (E_{abc_i} and I_{abc_i}) of DG_i are measured and then the Concordia transformation T_{32}^t is applied to those vectors which is then followed by the Park transformation $P(-\theta_i)$, and thus we obtain the voltage and current vectors (E_{dq_i} and I_{dq_i}). With the help of these vectors in dq frame, active and reactive power provided by DG_i is calculated. All the equations which resulted in the calculation are expressed in Eq. 3.7 and Eq. 3.8. To take into account the dynamics of the droop control of DG_i , a filter block is used with the power calculation block [5].

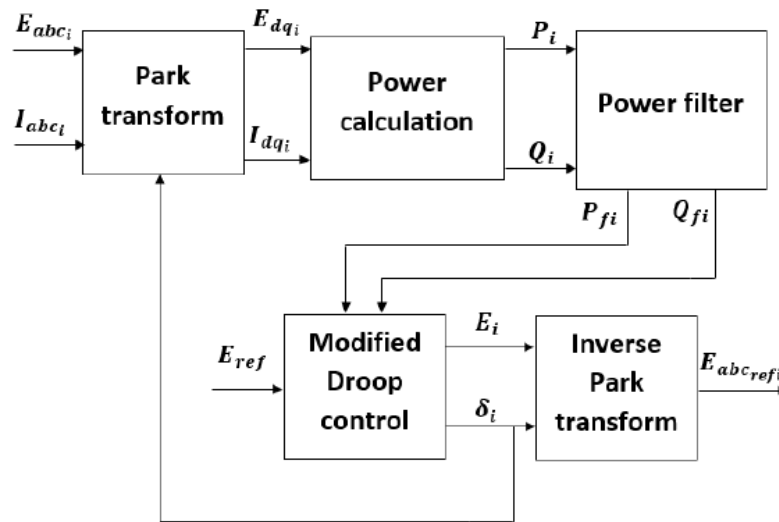


Figure 3.5 - Equivalent synoptic diagram describing a droop-controlled DG_i [5]

$$\begin{bmatrix} i_{di} \\ i_{qi} \end{bmatrix} = P(-\theta_i) T_{32}^t \begin{bmatrix} i_{ai} \\ i_{bi} \\ i_{ci} \end{bmatrix} = P(-\theta_i) T_{32}^t \begin{bmatrix} i_{ai} \\ i_{bi} \\ -i_{ai} - i_{bi} \end{bmatrix}$$

$$\begin{bmatrix} E_{di} \\ E_{qi} \end{bmatrix} = P(-\theta_i) T_{32}^t \begin{bmatrix} v_{ai} \\ v_{bi} \\ v_{ci} \end{bmatrix} = P(-\theta_i) T_{32}^t \begin{bmatrix} v_{aci} \\ v_{bci} \\ 0 \end{bmatrix}$$

$$T_{32}^t = \sqrt{\frac{2}{3}} \begin{bmatrix} 1 & -\frac{1}{2} & -\frac{1}{2} \\ 0 & \frac{\sqrt{3}}{2} & -\frac{\sqrt{3}}{2} \end{bmatrix}$$

$$P(\theta) = \begin{bmatrix} \cos \theta & -\sin \theta \\ \sin \theta & \cos \theta \end{bmatrix}$$

Where,

$$\theta_i = \int \omega_i dt$$

3.7

3.8

$$\begin{cases} P_i = E_{d_i} i_{d_i} + E_{q_i} i_{q_i} \\ Q_i = E_{q_i} i_{d_i} - E_{d_i} i_{q_i} \end{cases} \quad 3.9$$

Simulation Results

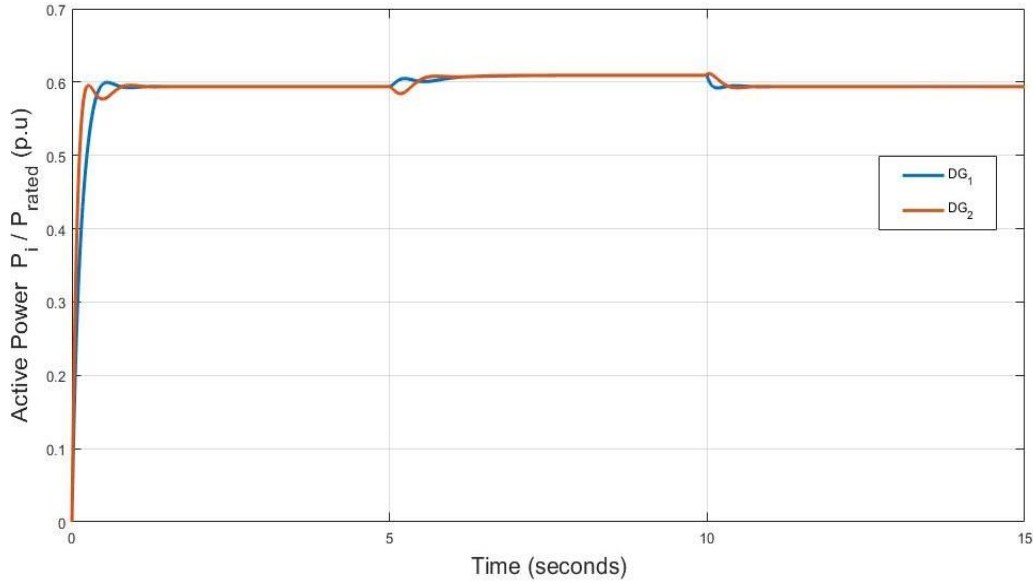


Figure 3.6 - Evolution of DGs active power

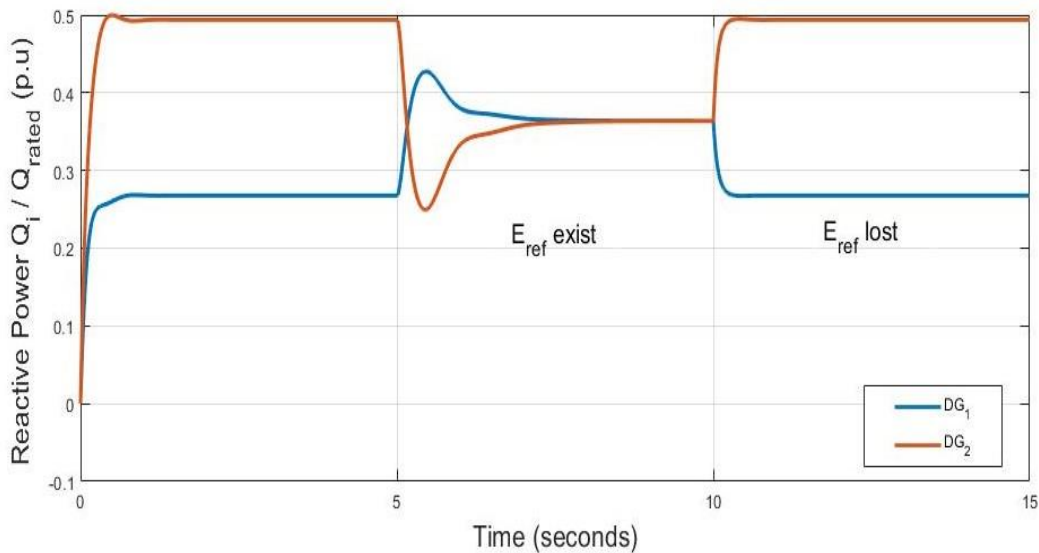


Figure 3.7 - Evolution of DGs reactive power

As it can be seen in Figure 3.6 that modification of droop control has no impact on active power sharing. However, as in Figure 3.7, it can be observed that the addition of the non-linear term $J_i(P_{fi} - P_{in})$ to the Q-V droop control resulted in accurate reactive power sharing between the DGs. But this modified Q-V droop control presents a few disadvantages and communication failure between DGs is one of them. If E_{ref} is not communicated to all DGs in the network for improving their voltages to have minimal voltage drop in the network, then it is not possible to achieve accurate reactive power sharing. Thus, it can be visualized in Figure 3.7 that when the communication of E_{ref} to the DGs is delayed or

lost, then reactive power sharing is also lost among the DGs. To avoid this centralized approach in Primary control, distributed approach is proposed which is discussed in detail in the next section where rather than communicating E_{ref} to all DGs in the network, DGs communicate with their neighboring DGs and try to achieve the same reference potential using a consensus approach.

3.2. Development of Distributed Primary Control Strategy - Using Consensus Theory

3.2.1. Modified Droop Control for Accurate Reactive Power Sharing

The modified control strategy proposed in section 3.1 results in accurate active and reactive power sharing in complex mesh MGs and its robustness is also verified by varying the load as well as changing the topology of the MG. However, when E_{ref} measured at the pilot node is not communicated properly to DGs in MG due to some error then reactive power sharing between DGs lost instantly. Therefore, this centralized approach to measuring E_{ref} and send to the local controllers of DGs will be omitted and instead new distributed control is proposed in this section using a consensus algorithm where DGs communicate with the neighboring DGs and their voltage values try to converge to the same value X_i which will be used in the non-linear control proposed in [5] instead of E_{ref} as explained in Eq. 3.12. The control becomes then as expressed in equations 3.10, 3.11, and 3.12.

$$\omega_i = \omega_n - m_i(P_{fi} - P_{in}) \quad 3.10$$

$$E_i = E_n - n_i(Q_{fi} - Q_{in}) + J'_i(P_{fi} - P_{in}) \quad 3.11$$

Where,

$$\left\{ \begin{array}{l} J'_i = K_i \int \varepsilon_i dt \\ \varepsilon_i = \left[-\alpha \left(\frac{X_i}{E_n} - 1 \right) + \left(\frac{Q_{fi}}{Q_{in}} - 1 \right) \right] \\ m_i = \frac{\Delta\omega}{P_{in}} \\ n_i = \frac{\Delta E}{Q_{in}} \end{array} \right. \quad 3.12$$

Network Graph and Associated Laplacian Matrix

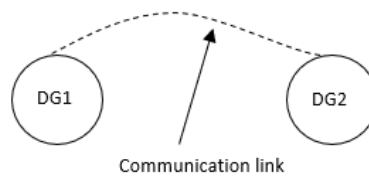


Figure 3.8 - Communication Link between two DGs in MG

$$\mathcal{L} = \begin{bmatrix} 1 & -1 \\ -1 & 1 \end{bmatrix}$$

Based on Figure 3.8, the Laplacian matrix can be formulated which describes the MG network. The terms in the diagonal of the matrix represent that DG_i is connected to how many neighboring links whereas the non-diagonal term represents the exact other DG to which DG_i is connected.

Determination of Reference Potential X_i Using Consensus Algorithm

Now, the consensus algorithm is going to be used as presented in Eq. 3.13 and 3.14 so that the reference potentials of the two DGs X_i converge to the same value. This method allows to get a common reference potential X_i which will be used in the non-linear control in equations 3.10, 3.11, and 3.12 which replaces the centralized control where E_{ref} is measured and then it has to be sent to all DGs by a global communication network.

$$\frac{d}{dt} \begin{bmatrix} X_1 \\ X_2 \end{bmatrix} = K_x \begin{bmatrix} E_1 - X_1 \\ E_2 - X_2 \end{bmatrix} - K_y \begin{bmatrix} Y_1 \\ Y_2 \end{bmatrix} \quad 3.13$$

$$\frac{d}{dt} \begin{bmatrix} Y_1 \\ Y_2 \end{bmatrix} = \mathcal{L} \begin{bmatrix} X_1 \\ X_2 \end{bmatrix} \quad 3.14$$

The proposed consensus algorithm is set so that the reference potentials of all the DGs (X_1 and X_2) converge to the same value in the steady state which is implanted using Eq. 3.14. Whereas Eq. **Error! Reference source not found.** set the dynamics meaning how the objective is going to be achieved.

Steady State Point

As it is known from Eq. 3.14

$$\frac{d}{dt} \begin{bmatrix} Y_1 \\ Y_2 \end{bmatrix} = \mathcal{L} \begin{bmatrix} X_1 \\ X_2 \end{bmatrix}$$

In a steady state,

$$\frac{d}{dt} \begin{bmatrix} Y_1 \\ Y_2 \end{bmatrix} = 0$$

So,

$$\mathcal{L} \begin{bmatrix} X_1 \\ X_2 \end{bmatrix} = 0$$

$$\begin{bmatrix} 1 & -1 \\ -1 & 1 \end{bmatrix} \begin{bmatrix} X_1 \\ X_2 \end{bmatrix} = 0$$

$$\begin{bmatrix} X_1 & -X_2 \\ -X_1 & X_2 \end{bmatrix} = 0$$

$$X_1 - X_2 = 0$$

$$X_1 = X_2$$

Design of Parameters K_x and K_y for the measurement of the common potential:

To propose a design of the control parameters independent of the MG parameters or topology, the dynamic of the state variable X_i is designed in such a way that it has to be slow as compared to the

dynamic bound to integral term J_i . Thus, ε_i is supposed to be null. 3.13 and 3.14 being linear equations can be written as:

$$\frac{d}{dt} X = k_x[E - X] - k_y Y$$

$$\frac{d}{dt} Y = \mathcal{L}Y$$

Taking Laplace's transformation, we get:

$$sX = k_x[E - X] - k_y Y \quad 3.15$$

$$sY = \mathcal{L}Y$$

$$Y = \frac{\mathcal{L}X}{s} \quad 3.16$$

Substituting Eq. 3.16 in 3.15, we get:

$$sX = k_x[E - X] - k_y \frac{\mathcal{L}X}{s}$$

$$sX = \frac{sk_x[E - X] - k_y \mathcal{L}X}{s}$$

$$s^2 X = sk_x[E - X] - k_y \mathcal{L}X$$

$$s^2 X + sk_x X + k_y \mathcal{L}X = sk_x E$$

$$(s^2 + sk_x + k_y \mathcal{L})X = sk_x E$$

We define K_x and K_y as diagonal matrices which are equal respectively to $K_x I_3$ and $K_y I_3$. By evaluating zeros of $P(s)$, the poles of the system are determined as follows:

$$P(s) = \det[s^2 + sk_x + k_y \mathcal{L}]$$

A pole placement procedure is used to determine the values of K_x and K_y which is identical for all DGs. The design of parameters is dependent on the knowledge of the Laplacian matrix but the implementation of the control law is distributed.

Simulation Results

- **At 5 sec:** The proposed consensus-based non-linear control for power sharing as shown in Eq. 3.11 is applied.
- **At 10 sec:** One of the loads is disconnected.
- **At 15 sec:** One of the power lines is disconnected.

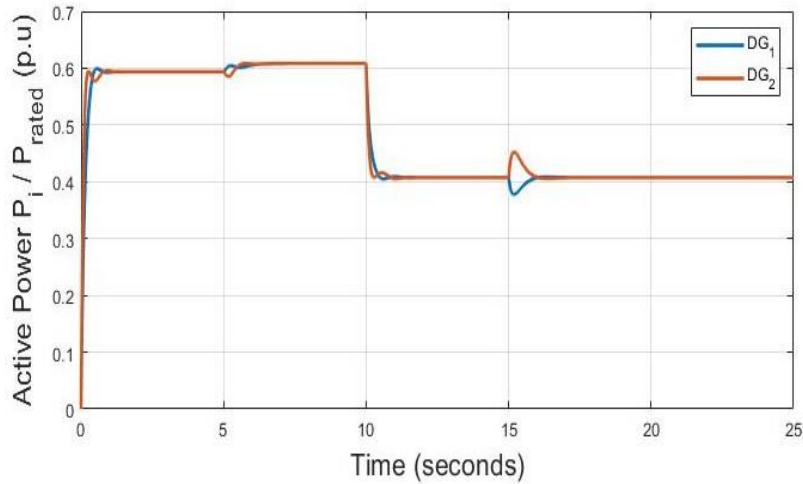


Figure 3.9 - Evolution of DGs active power (using consensus approach)

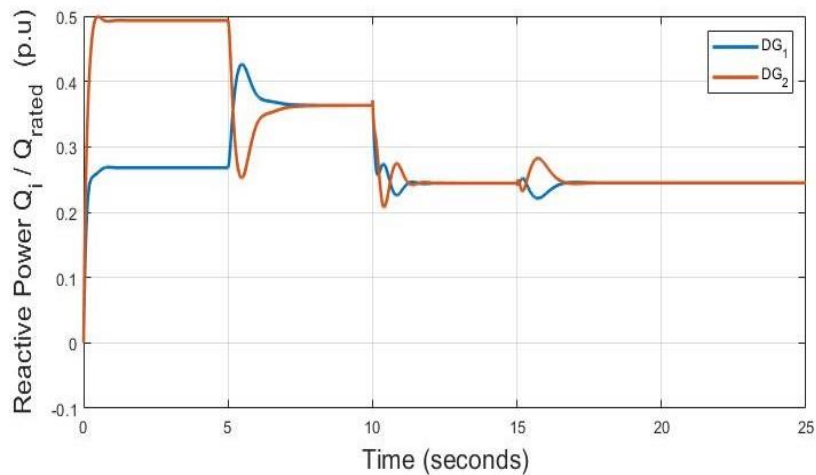


Figure 3.10 - Evolution of DGs reactive power (using consensus approach)

In Figure 3.9, the evolution of the active power of both DGs can be observed. After 5 sec when the non-linear control is added to the Q-V droop control, it does not show any effect on the active power sharing which is achieved by $P - \omega$ droop control. The robustness of the proposed control strategy has been tested and it can be seen that when the load and power line are disconnected at 10 and 15 sec respectively, the power output by both DGs is adjusted accordingly and results in equal active power sharing throughout the time.

In Figure 3.10, the evolution of the reactive power of both DGs can be seen. At 5 sec, due to the addition of non-linear control to the conventional Q-V droop control, the voltage profile of the overall network is improved which resulted in lower losses in the network, and hence, resulted in accurate reactive power sharing between the DGs. To check the robustness of the proposed control strategy, load and power lines are disconnected at 10 and 15 sec respectively, but an accurate reactive power sharing is observed after those changes in the network, which ensures the robustness of the developed control strategy.

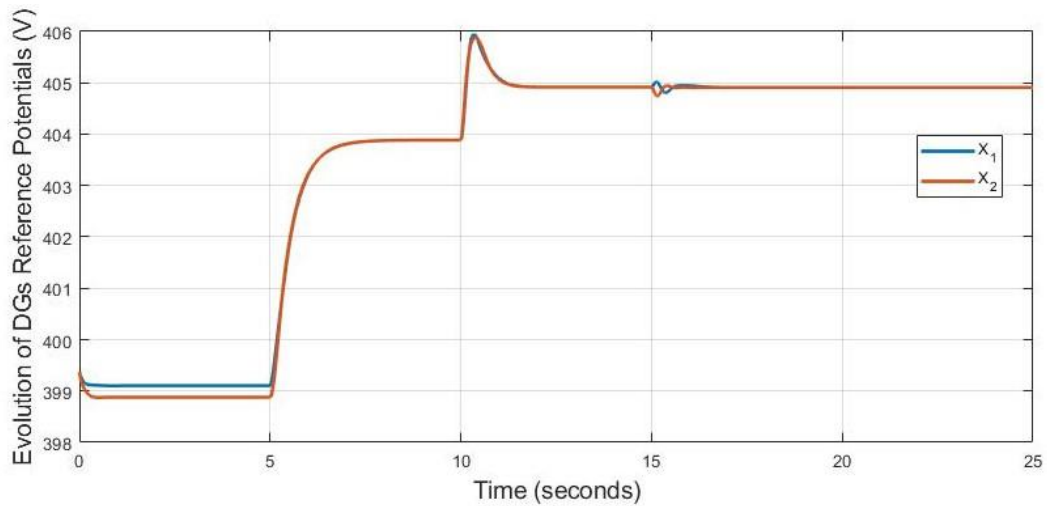


Figure 3.11 - Evolution of DGs Reference Potential

In Figure 3.11, it can be observed that both DGs communicate with each other and achieve the same reference potential X_i after 5 sec when control strategy based on a consensus approach is applied to the network.

Problems arise as a result of Primary control

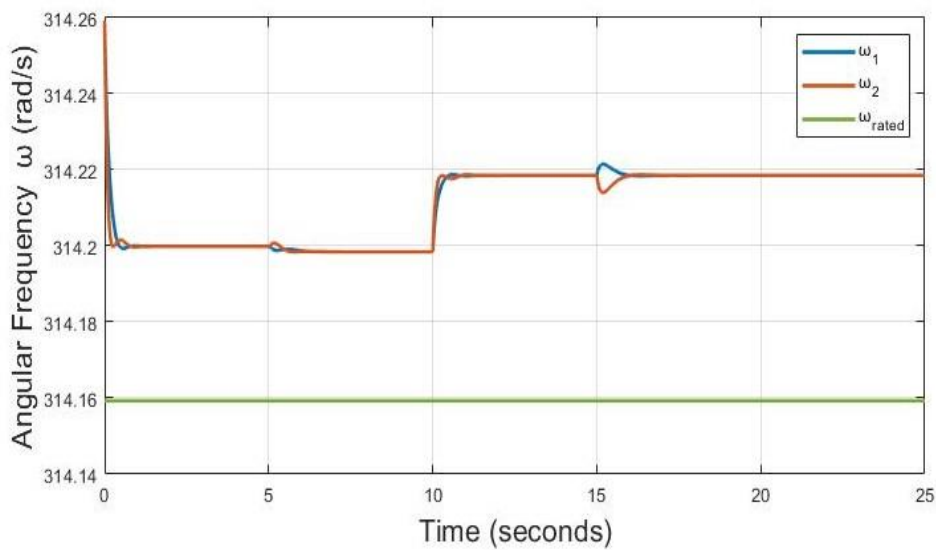


Figure 3.12 - Deviation of DGs frequency from the rated frequency

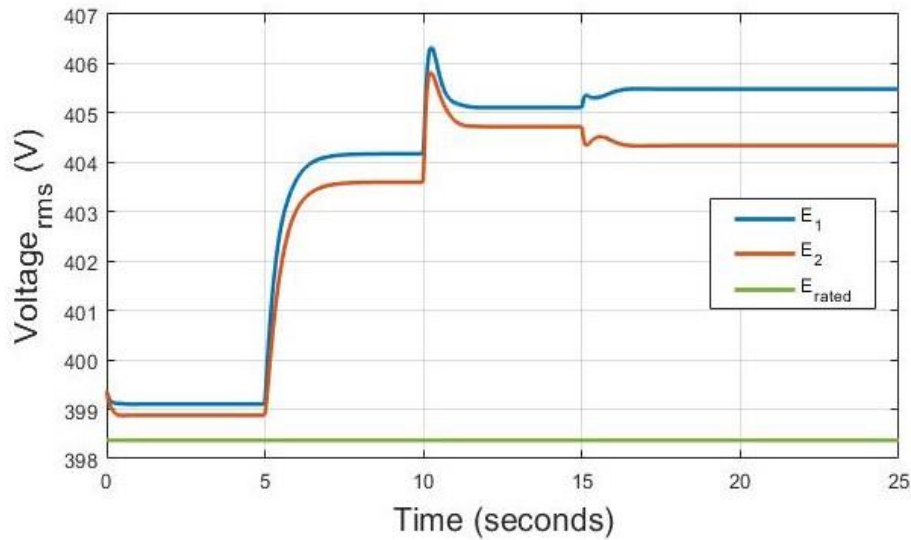


Figure 3.13 - Deviation of DGs voltage from the rated voltage

Due to primary control and addition of the non-linear term as seen in Eq. 3.11, the voltage and frequency of both DGs deviated from their rated value which is not suitable for the load and other equipment connected in the network as voltage and frequency should remain within a certain range of rated values for the proper functioning of the power system.

It can be observed in Figure 3.12 that the angular frequency of both DGs deviated from the rated frequency and in Figure 3.13, it can be observed that the voltage values of both DGs are not following the rated value anymore. This deviation can be resolved by the implementation of secondary control strategy on the mesh-type AC microgrid which is discussed in the next section.

3.3. Development of Distributed Secondary Control Strategies – Using Consensus

3.3.1. Restoration of DGs Frequency to Rated Frequency

The objective of secondary control is to bring the Voltage and frequency of DGs back to rated values which are affected by accurate power sharing achieved by the primary control. However, it must be ensured that secondary control does not in any way affect active and reactive power sharing between DGs.

Using the consensus-based control expressed in equations 3.17, 3.18, and 3.19, the distributed control proposed in this section aims to force all DGs frequencies to converge to the same value while forcing the errors $(\omega_i - \omega_n)$ to zero. This allows the restoration of frequencies of both DGs to their rated values without affecting their active power sharing. The frequency droop controller is modified where the term X_{ω_i} defined by Eq. 3.20 is added to Eq. 3.10 to obtain the new frequency Droop control given by Eq. 3.17.

$$\frac{d\omega_i}{dt} = \omega_f(-\omega_i + \omega_n - m_i(P_i - P_{in}) - X_{\omega_i}) \quad 3.17$$

$$\frac{dE_i}{dt} = \omega_f \left(-E_i + E_n - \frac{\Delta_E}{Q_{in}}(Q_i - Q_{in}) - J_i(P_i - P_{in}) \right) \quad 3.18$$

Where,

$$J'_i = K_i \int \varepsilon_i dt$$

$$\varepsilon_i = \left[-\alpha \left(\frac{X_i}{E_n} - 1 \right) + \left(\frac{Q_{fi}}{Q_{in}} - 1 \right) \right]$$
3.19

Now for distributed control approach:

$$\frac{d}{dt} X_\omega = -\mathcal{L}K_1 X_\omega + K_2(\omega - \omega_n I_2)$$
3.20

With:

$$I_2 = \begin{bmatrix} 1 \\ 1 \end{bmatrix}$$

$$X_\omega = \begin{bmatrix} X_{\omega 1} \\ X_{\omega 2} \end{bmatrix}$$

$$\omega = \begin{bmatrix} \omega_1 \\ \omega_2 \end{bmatrix}$$

$$\{K_1, K_2\} \in \mathbb{R}^2$$

We know that if the system is stable then X_ω reaches a steady state point, then $\frac{d}{dt} X_\omega = 0$.

Thus, Using Eq. 3.20:

$$\frac{d}{dt} X_\omega = -\mathcal{L}K_1 X_\omega + K_2(\omega - \omega_n I_2)$$

$$0 = -\mathcal{L}K_1 X_\omega + K_2(\omega - \omega_n I_2)$$

Multiply Both sides by I^t ,

$$0 = -I^t \mathcal{L}K_1 X_\omega + I^t K_2(\omega - \omega_n I_2)$$

Use property: $I^t \cdot \mathcal{L} = 0$

$$0 = 0 + I^t K_2(\omega - \omega_n I_2)$$

$$0 = I^t K_2(\omega - \omega_n I_2)$$

$$0 = (\omega - \omega_n I_2)$$

$$\omega = \omega_n I_2$$

$$\begin{bmatrix} \omega_1 \\ \omega_2 \end{bmatrix} = \begin{bmatrix} \omega_n \\ \omega_n \end{bmatrix}$$

Thus,

$$\omega_1 = \omega_2 = \omega_n$$
3.21

Eq. 3.21 shows that this distributed control law ensures frequency restoration to the rated value if asymptotic stability is ensured.

Design of Parameters K_1 and K_2

The design of parameters of the controller for secondary frequency control is based on separating its dynamics from the ones of the primary control. The primary control loop should be fast as compared

to the secondary which means first DGs impose Voltage and frequency in grid forming mode to the whole MG, achieve power sharing, and then secondary control brings voltage and frequency of DGs back to the rated values.

From Eq. 3.17

$$\frac{d\omega_i}{dt} = \omega_f(-\omega_i + \omega_n - m_i(P_i - P_{in}) - X_{\omega i})$$

An assumption has been made that the dynamic of the primary controller is widely faster than the dynamic of the secondary controller. So, we suppose that $\frac{d\omega_i}{dt} = 0$

So:

$$0 = (-\omega_i + \omega_n - m_i(P_i - P_{in}) - X_{\omega i})$$

$$\omega_i = \omega_n - m_i(P_i - P_{in}) - X_{\omega i}$$

But,

$$m_i = \frac{\Delta\omega}{P_{in}}$$

So,

$$\omega_i = \omega_n - \frac{\Delta\omega}{P_{in}}(P_i - P_{in}) - X_{\omega i}$$

Now,

$$\frac{\Delta\omega}{P_{in}}(P_i - P_{in}) = \gamma$$

So,

$$\omega_i = \omega_n - \gamma - X_{\omega i} \quad 3.22$$

From Eq. 3.20, we know that

$$\frac{d}{dt}X_{\omega} = -\mathcal{L}K_1X_{\omega} + K_2(\omega_i - \omega_n I_2)$$

Using ω_i from equation 3.22,

$$\frac{d}{dt}X_{\omega} = -\mathcal{L}K_1X_{\omega} + K_2(\omega_n I_2 - \gamma I_2 - X_{\omega i} - \omega_n I_2)$$

$$\frac{d}{dt}X_{\omega} = -\mathcal{L}K_1X_{\omega} + -\gamma I_2 K_2 - K_2 X_{\omega i}$$

In a steady state, $\frac{d}{dt}X_{\omega} = 0$, so:

$$0 = -\mathcal{L}K_1X_{\omega} - \gamma I_2 K_2 - K_2 X_{\omega i}$$

Multiply Both sides by I^t ,

$$0 = -I^t \mathcal{L}K_1X_{\omega} - I^t \gamma I_2 K_2 - I^t K_2 X_{\omega i}$$

Use property: $I^t \cdot \mathcal{L} = 0$

$$0 = 0 - I^t I_2 \gamma K_2 - I^t K_2 X_{\omega i}$$

$$0 = 0 - 2 \gamma K_2 - I^t K_2 X_{\omega i}$$

$$I^t K_2 X_{\omega i} = -2 \gamma K_2$$

$$I^t X_{\omega i} = -2 \gamma$$

In the Steady state, both DGs have the same value of X_{ω} which shows that power-sharing will not be affected by the imposition of secondary control in the MG.

The parameters K_1 and K_2 are designed thanks to a pole placement process. The associated bandwidth is kept 10 times lower than the bandwidth of the primary controller with its consensus-based distributed controller. $K_1=0.01$ and $K_2=0.1$ which corresponds to a bandwidth equal to 0.1 rad/s.

Simulation Results

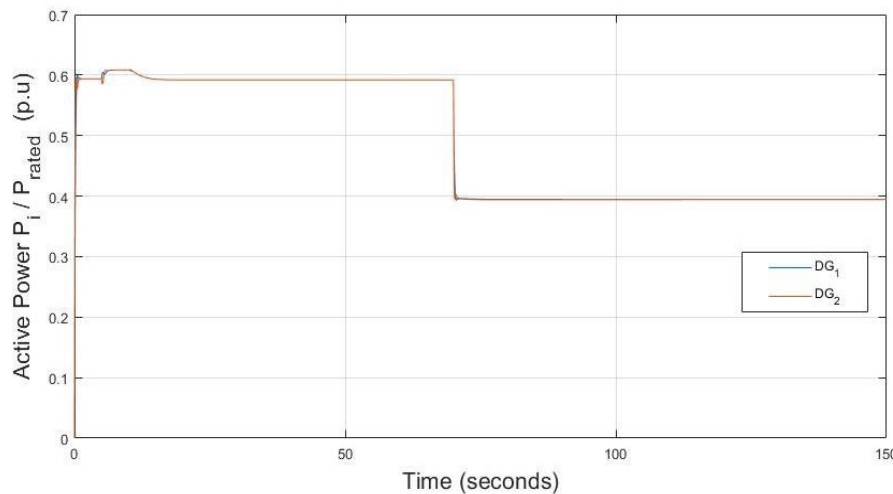


Figure 3.14 - Evolution of DGs active power

As can be observed in Figure 3.14 the implementation of the secondary control strategy has not in any way affected the active power sharing among the DGs. The response time of secondary control is set to be 50 sec after implementation of primary control which can be observed in this figure, as at 5 sec, primary control has been implemented and then secondary control takes 50 sec as response time to restore frequencies of DGs to the rated values. As can be seen in Figure 3.16 that between 5 to 55 sec, the angular frequencies of both DGs try to approach the rated value.

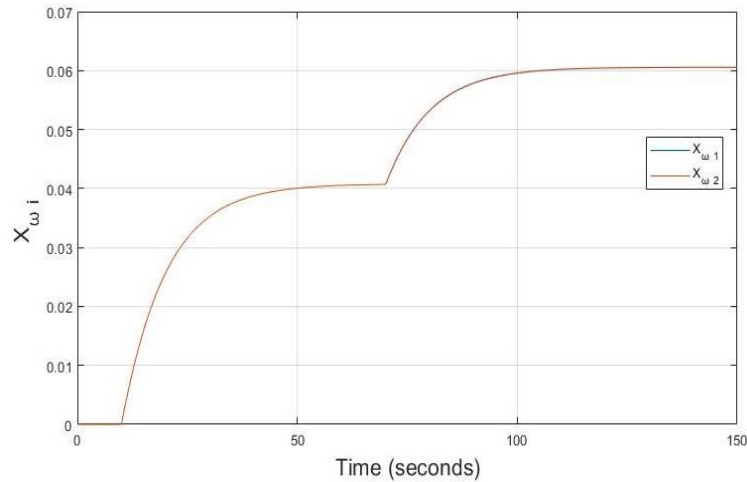
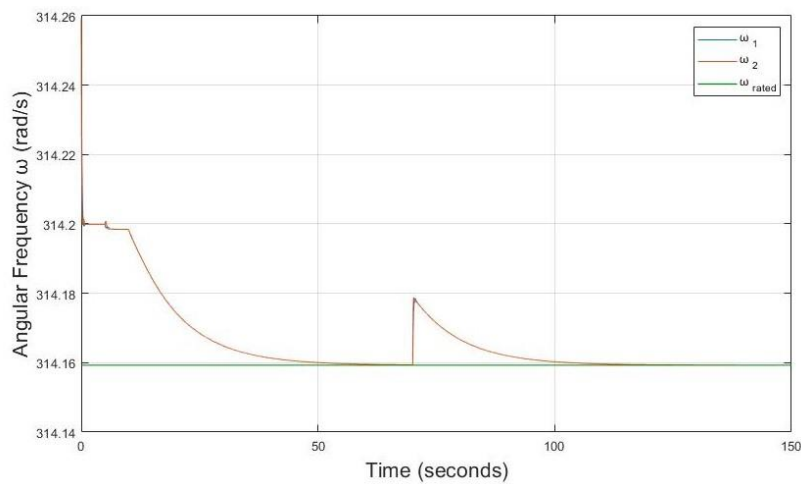
Figure 3.15 - Evolution of X_{ω_i} of DGs

Figure 3.16 - Restoration of DGs frequency to the rated frequency

In Figure 3.16, it can be seen that when secondary control is implemented after 5 sec, the angular frequency of both DGs approach the rated value of frequency which is also proved mathematically as in Eq. 3.21.

3.3.2. Restoration of DGs Voltage Close to Rated Voltage

The distributed control proposed in equations 3.23 and 3.24 aims to force the average voltage of two DGs to converge to the rated voltage E_n while keeping the DGs reactive power sharing accurate which is achieved by the primary control. To maintain the equal sharing of the reactive power between the DGs in MG, the additional term X_{vi} has been the same for all DGs in the steady state. This property is achieved by using the distributed control law as expressed in equation 3.26. In Eq. 3.26 we determine X_{vi} which is added to the nonlinear coefficient J'_i in 3.19 making it J''_i for reactive power sharing in Eq. 3.25.

$$\frac{d\omega_i}{dt} = \omega_f(-\omega_i + \omega_n - m_i(P_i - P_{in}) - X_{\omega i}) \quad 3.23$$

$$\frac{dE_i}{dt} = \omega_f(-E_i + E_n - \frac{\Delta E}{Q_{in}}(Q_i - Q_{in}) - J''_i(P_i - P_{in})) \quad 3.24$$

With:

$$\left\{ \begin{array}{l} J''_i = K_i \int \varepsilon_i dt \\ \varepsilon_i = \left[-\alpha \left(\frac{X_i}{E_n} - 1 \right) - \left(\frac{Q_i}{Q_{in}} - 1 \right) \right] - X_{vi} \end{array} \right. \quad 3.25$$

From consensus,

$$\frac{dX_v}{dt} = -f_2 \mathcal{L} X_v + f(X - E_n) \quad 3.26$$

With:

$$(f_2, f) \in \mathbb{R}^2, \\ X_v = \begin{bmatrix} X_{v1} \\ X_{v2} \\ X_{v3} \end{bmatrix}$$

Steady State Point

From distributed primary control as expressed in equations 3.13 and 3.14, we know that

$$\frac{d}{dt} \begin{bmatrix} X_1 \\ X_2 \end{bmatrix} = K_x \begin{bmatrix} E_1 - X_1 \\ E_2 - X_2 \end{bmatrix} - K_y \begin{bmatrix} Y_1 \\ Y_2 \end{bmatrix} \\ \frac{d}{dt} Y = \mathcal{L} \begin{bmatrix} X_1 \\ X_2 \end{bmatrix}$$

Multiply both sides by I^t

$$\frac{d}{dt} I^t Y = I^t \mathcal{L} X$$

Use property: $I^t \cdot \mathcal{L} = 0$

$$\frac{d}{dt} I^t Y = 0$$

A derivative is zero means Y is constant. And the value of the constant is also zero.

$$I^t Y = 0$$

An assumption has been made that the dynamic of the primary controller is widely faster than the dynamic of the secondary controller. So, we suppose that $\frac{d}{dt} X = 0$.

So, using Eq. 3.13:

$$\frac{d}{dt} X = K_x[E - X] - K_y Y \\ 0 = K_x[E - X] - K_y Y$$

Multiply both sides by I^t

$$0 = K_x I^t [E - X] - K_y I^t Y$$

As we know,

$$I^t Y = 0$$

So,

$$0 = K_x I^t [E - X] - 0$$

$$0 = I^t [E - X] \quad 3.27$$

From Eq. 3.27, it is concluded that all components of X are equal to E.

Now, from distributed secondary control based on consensus as expressed in Eq. 3.26, we know that:

$$\frac{d}{dt} X_v = -f_2 \mathcal{L} X_v + f(X - E_n)$$

In the Steady state, $dX_v = 0$

$$0 = -f_2 \mathcal{L} X_v + f(X - E_n)$$

Multiply both sides by I^t

$$0 = -f_2 I^t \mathcal{L} X_v + f I^t (X - E_n)$$

Use property: $I^t \cdot \mathcal{L} = 0$

$$0 = -0 + f I^t (X - E_n)$$

$$0 = f I^t (X - E_n)$$

$$0 = I^t (X - E_n)$$

$$I^t X = I^t E_n$$

$$\begin{bmatrix} X_1 \\ X_2 \end{bmatrix} = \begin{bmatrix} E_n \\ E_n \end{bmatrix}$$

From primary consensus, we know that, the reference potential X_i of both DGs converge to the same value. Thus, it can be written as:

$$X_1 = X_2 = X$$

So,

$$\begin{bmatrix} X \\ X \end{bmatrix} = \begin{bmatrix} E_n \\ E_n \end{bmatrix}$$

Thus,

$$X = E_n$$

From the above equation, it can be concluded that X converges to the rated value of voltage E_n .

Now coming back to Eq. 3.27,

$$0 = I^t [E - X]$$

$$I^t E = I^t X$$

From the above equation, it can be observed that the average value of voltages of two DGs converges to X which can be written mathematically as follows:

$$E_1 + E_2 = 2 X$$

$$\frac{E_1 + E_2}{2} = X$$

But we know that X converges to the rated value of voltage E_n .

So,

$$\frac{E_1 + E_2}{2} = E_n \quad 3.28$$

Thus, it is mathematically proved from Eq. 3.28 that the average value of voltages of both DGs converge to the rated value of voltage E_n .

Design of Parameters f and f_2

The design of parameters of the controller for secondary voltage control is based on separating its dynamics from the ones of the primary control. The primary control loop should be fast as compared to the secondary which means first DGs impose Voltage and frequency in grid forming mode to the whole MG, achieve power sharing, and then secondary control brings voltage and frequency of DGs back to the rated values.

From Eq. 3.26, we know that:

$$dX_v = -f_2 \mathcal{L}X_v + f(X - E_n)$$

Using Eq. 3.25,

$$\varepsilon_i = \left[-\alpha \left(\frac{X_i}{E_n} - 1 \right) - \left(\frac{Q_i}{Q_{in}} - 1 \right) \right] - X_v$$

In the Steady state, $\varepsilon_i = 0$ so,

$$0 = \left[-\alpha \left(\frac{X_i}{E_n} - 1 \right) - \left(\frac{Q_i}{Q_{in}} - 1 \right) \right] - X_v$$

$$X_v = \left[-\alpha \left(\frac{X_i}{E_n} - 1 \right) - \left(\frac{Q_i}{Q_{in}} - 1 \right) \right]$$

$$X_v = -\alpha \left(\frac{X_i - E_n}{E_n} \right) - \left(\frac{Q_i}{Q_{in}} - 1 \right)$$

$$X_v + \left(\frac{Q_i}{Q_{in}} - 1 \right) = -\frac{\alpha}{E_n} (X_i - E_n)$$

$$-\frac{E_n}{\alpha} \left[X_v + \left(\frac{Q_i}{Q_{in}} - 1 \right) \right] = (X_i - E_n) \quad 3.29$$

Putting value of $(X_i - E_n)$ from Eq. 3.29 to 3.26, we get:

$$dX_v = -f_2 \mathcal{L}X_v - \frac{f E_n}{\alpha} \left[X_v + \left(\frac{Q_i}{Q_{in}} - 1 \right) \right]$$

$$dX_v = -f_2 \mathcal{L} X_v - \frac{f E_n X_v}{\alpha} - \frac{f E_n}{\alpha} \left(\frac{Q_i}{Q_{in}} - 1 \right)$$

$$dX_v + f_2 \mathcal{L} X_v + \frac{f E_n X_v}{\alpha} = - \frac{f E_n}{\alpha} \left(\frac{Q_i}{Q_{in}} - 1 \right)$$

Taking Laplace transform, we get:

$$sX_v + f_2 \mathcal{L} X_v + \frac{f E_n X_v}{\alpha} = - \frac{f E_n}{\alpha} \left(\frac{Q_i}{Q_{in}} - 1 \right)$$

$$\left[s + f_2 \mathcal{L} + \frac{f E_n}{\alpha} \right] X_v = - \frac{f E_n}{\alpha} \left(\frac{Q_i}{Q_{in}} - 1 \right)$$

Simulation Results

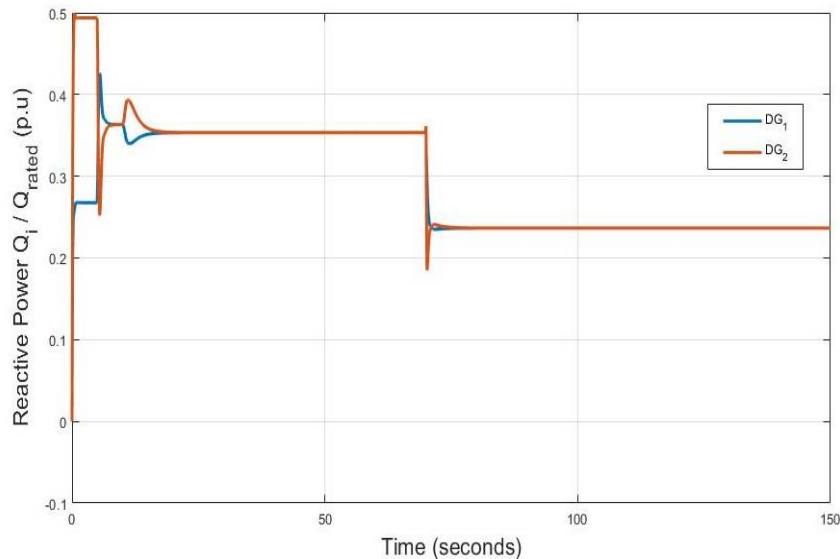


Figure 3.17 - Evolution of DGs reactive power (using consensus approach)

As can be observed in Figure 3.17 the implementation of the secondary control strategy has not in any way affected the reactive power sharing among both the DGs. The response time of secondary control is set to be 50 sec after implementation of primary control which can be observed in the figure, as at 5-sec primary control has been implemented and then secondary control takes 50 sec as response time to restore voltages close to the rated values.

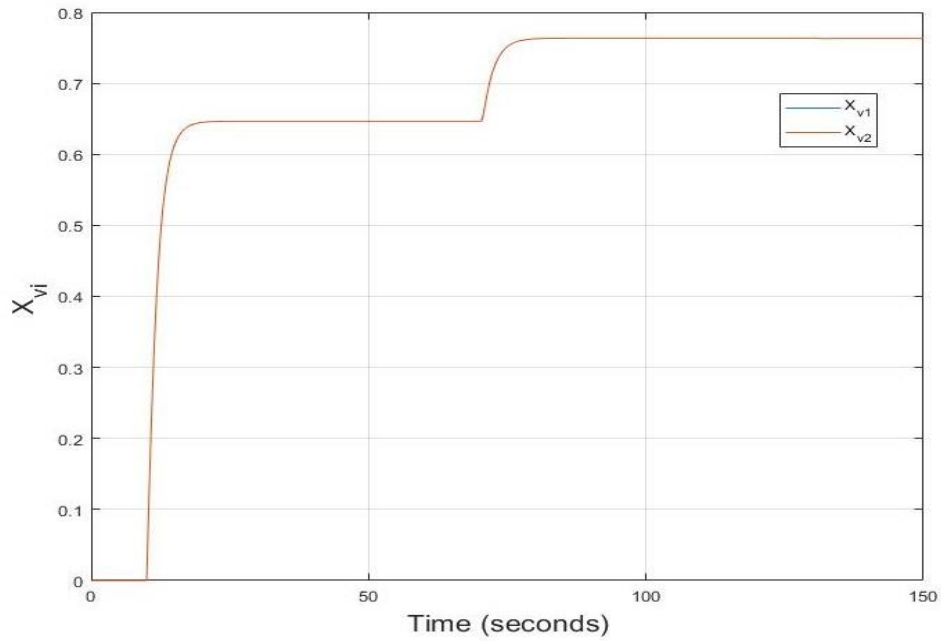
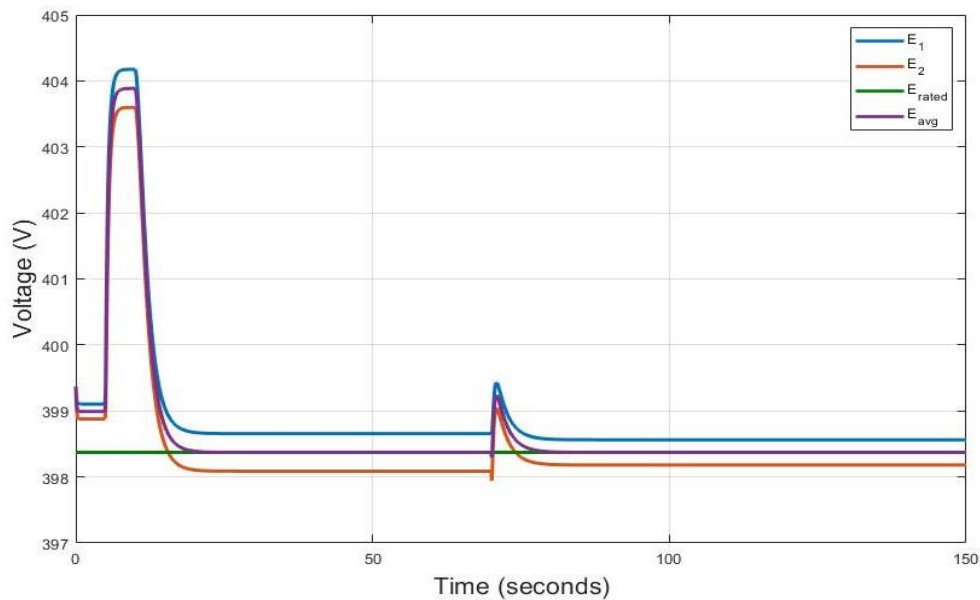
Figure 3.18 - Evolution of X_{vi} of DGs

Figure 3.19 - Average voltage of DGs approach the rated voltage

In Figure 3.19, it can be seen that when secondary control is implemented after 5 sec, the average voltages of both DGs approach the rated value which is also proved mathematically as in Eq. 3.28.

Conclusion

As discussed in the Literature review section that various topologies exist for microgrids (MGs) such as mono-PCC simple MG or multi-PCC mesh-type MG. To avoid the problems of overstress and aging of DG sources integrated into MG, it is necessary to achieve accurate active and reactive power sharing among them. For this purpose, conventional droop control methods $P - \omega$ and Q-V are implemented in these MGs for efficient and accurate power sharing. $P - \omega$ droop control method works very well for simple as well as complex topologies of MGs. However, conventional Q-V droop control does not result in accurate reactive power sharing among the DGs in complex MG topologies such as mesh-type MG. The prominent reason is that in complex MG topologies, power lines offer non-neglectable resistances and inductances which results in the voltage drop in the overall network, and this originates the power coupling phenomena in the network where active and reactive power is coupled. This coupling does not allow accurate reactive power sharing with the implementation of the traditional Q-V droop control method.

In literature, several methods have been proposed by different authors. One of them has been discussed in this report where conventional Q-V droop control has been modified by adding a non-linear term which results in the decoupling of active and reactive power and results in accurate reactive power sharing [5]. However, the control strategy developed and implemented in [5] is based on a centralized approach where reference potential E_{ref} is measured at the pilot node of the network and communicated to all DGs present in the network. All the DGs adjust their voltage values based on that reference potential E_{ref} . The most important disadvantage associated with this approach which is also verified from simulations result is that if there is communication failure in the network and E_{ref} is not communicated to the DGs then ultimately reactive power sharing is lost.

Considering this thing, modifications have been made in the control approach. Distributed control approach based on a consensus algorithm is adopted and implemented in modified Q-V droop control with the non-linear term. This resulted in accurate power sharing among DGs without the need for global communication. But this primary control results in deviation of frequency and voltage values of all DGs from their rated values. Thus, secondary control is implemented which results in the restoration of frequency and voltage values of all DGs in the network to their rated values but special parameters have been introduced in the secondary control to make sure that it does not in any way affect the power-sharing achieved through primary control.

The objectives achieved during this project are summarized as follows:

- A consensus-based non-linear distributed control strategy for Primary control in islanded mesh microgrids is proposed.
- It ensures DGs active and reactive power sharing for mesh AC microgrids.
- A consensus-based non-linear distributed control strategy for Secondary control in islanded mesh microgrids is proposed.
- It ensures restoration of DGs frequency and voltage to their rated values or close to rated values.
- The simulation results confirm the efficiency of the proposed control as well as its robustness concerning load variations and topology changes.

References

- [1] T. Lam Nguyen, "Agent-based distributed control and optimization in microgrids with Hardware-in-the-Loop implementation", Accessed: Jun. 16, 2022. [Online]. Available: <https://tel.archives-ouvertes.fr/tel-02413611>
- [2] E. Planas, A. Gil-De-Muro, J. Andreu, I. Kortabarria, and I. Martínez De Alegría, "General aspects, hierarchical controls and droop methods in microgrids: A review," *Renewable and Sustainable Energy Reviews*, vol. 17, pp. 147–159, Jan. 2013, doi: 10.1016/J.RSER.2012.09.032.
- [3] H. Bevrani, B. François, and T. Ise, *Microgrid dynamics and control*.
- [4] Y. Hennane, A. Berdai, J. P. Martin, S. Pierfederici, and F. Meibody-Tabar, "New Decentralized Control of Mesh AC Microgrids: Study, Stability, and Robustness Analysis," *Sustainability*, vol. 13, no. 4, p. 2243, Feb. 2021, doi: 10.3390/SU13042243.
- [5] Y. Hennane, A. Berdai, S. Pierfederici, F. Meibody-Tabar, and J. P. Martin, "Novel non-linear control for synchronization and power sharing in islanded and grid-connected mesh microgrids," *Electric Power Systems Research*, vol. 208, Jul. 2022, doi: 10.1016/J.EPSR.2022.107869.
- [6] K. de Brabandere, B. Bolsens, J. van den Keybus, A. Woyte, J. Driesen, and R. Belmans, "A voltage and frequency droop control method for parallel inverters," *IEEE Trans Power Electron*, vol. 22, no. 4, pp. 1107–1115, Jul. 2007, doi: 10.1109/TPEL.2007.900456.
- [7] H. Mahmood, D. Michaelson, and J. Jiang, "Accurate Reactive Power Sharing in an Islanded Microgrid Using Adaptive Virtual Impedances," *undefined*, vol. 30, no. 3, pp. 1605–1617, 2015, doi: 10.1109/TPEL.2014.2314721.
- [8] J. Jiao, S. Guo, C. Tan, Y. Xue, and X. Hua, "Research on Improved Droop Control Method of DC Microgrid Based on Voltage Compensation," *2020 5th International Conference on Power and Renewable Energy, ICPRE 2020*, pp. 391–395, Sep. 2020, doi: 10.1109/ICPRE51194.2020.9233216.
- [9] "Distributed cooperative control for DC microgrids - Archive ouverte HAL." <https://hal.archives-ouvertes.fr/tel-03188133/> (accessed Aug. 22, 2022).
- [10] T. Dragicevic, X. Lu, J. C. Vasquez, and J. M. Guerrero, "DC Microgrids—Part I: A Review of Control Strategies and Stabilization Techniques," *IEEE Trans Power Electron*, vol. 31, no. 7, pp. 1–1, Jul. 2015, doi: 10.1109/TPEL.2015.2478859.
- [11] F. Blaabjerg, "Control of power electronic converters and systems. Volume 3".
- [12] J. Rocabert, A. Luna, F. Blaabjerg, and P. Rodríguez, "Control of power converters in AC microgrids," *IEEE Trans Power Electron*, vol. 27, no. 11, pp. 4734–4749, 2012, doi: 10.1109/TPEL.2012.2199334.
- [13] F. Z. Peng, Y. W. Li, and L. M. Tolbert, "Control and protection of power electronics interfaced distributed generation systems in a customer-driven microgrid," *2009 IEEE Power and Energy Society General Meeting, PES '09*, 2009, doi: 10.1109/PES.2009.5275191.

- [14] Y. Li, D. M. Vilathgamuwa, and P. C. Loh, "Design, analysis, and real-time testing of a controller for multibus microgrid system," *IEEE Trans Power Electron*, vol. 19, no. 5, pp. 1195–1204, Sep. 2004, doi: 10.1109/TPEL.2004.833456.
- [15] M. C. Chandorkar, D. M. Divan, and R. Adapa, "Control of parallel connected inverters in standalone ac supply systems," *IEEE Trans Ind Appl*, vol. 29, no. 1, pp. 136–143, 1993, doi: 10.1109/28.195899.
- [16] "A Comparison of Grid-Forming and Grid-Following Control of VSCs." <http://www.diva-portal.org/smash/record.jsf?pid=diva2%3A1444307&dswid=-5558> (accessed Jun. 20, 2022).
- [17] D. E. Olivares *et al.*, "Trends in microgrid control," *IEEE Trans Smart Grid*, vol. 5, no. 4, pp. 1905–1919, 2014, doi: 10.1109/TSG.2013.2295514.
- [18] H. Karimi, H. Nikkhajoei, and R. Iravani, "Control of an electronically-coupled distributed resource unit subsequent to an islanding event," *IEEE Transactions on Power Delivery*, vol. 23, no. 1, pp. 493–501, Jan. 2008, doi: 10.1109/TPWRD.2007.911189.
- [19] F. Katiraei, M. R. Iravani, and P. W. Lehn, "Micro-grid autonomous operation during and subsequent to islanding process," *IEEE Transactions on Power Delivery*, vol. 20, no. 1, pp. 248–257, Jan. 2005, doi: 10.1109/TPWRD.2004.835051.
- [20] J. A. P. Lopes, C. L. Moreira, and A. G. Madureira, "Defining control strategies for microgrids islanded operation," *IEEE Transactions on Power Systems*, vol. 21, no. 2, pp. 916–924, May 2006, doi: 10.1109/TPWRS.2006.873018.
- [21] F. Blaabjerg, R. Teodorescu, M. Liserre, and A. v. Timbus, "Overview of control and grid synchronization for distributed power generation systems," *IEEE Transactions on Industrial Electronics*, vol. 53, no. 5, pp. 1398–1409, Oct. 2006, doi: 10.1109/TIE.2006.881997.
- [22] F. Gao and M. R. Iravani, "A control strategy for a distributed generation unit in grid-connected and autonomous modes of operation," *IEEE Transactions on Power Delivery*, vol. 23, no. 2, pp. 850–859, Apr. 2008, doi: 10.1109/TPWRD.2007.915950.
- [23] M. C. Chandorkar, D. M. Divan, and R. Adapa, "Control of parallel connected inverters in standalone ac supply systems," *IEEE Trans Ind Appl*, vol. 29, no. 1, pp. 136–143, 1993, doi: 10.1109/28.195899.
- [24] A. Bidram and A. Davoudi, "Hierarchical structure of microgrids control system," *IEEE Trans Smart Grid*, vol. 3, no. 4, pp. 1963–1976, 2012, doi: 10.1109/TSG.2012.2197425.
- [25] Y. Levron, J. M. Guerrero, and Y. Beck, "Optimal power flow in microgrids with energy storage," *IEEE Transactions on Power Systems*, vol. 28, no. 3, pp. 3226–3234, 2013, doi: 10.1109/TPWRS.2013.2245925.
- [26] F. Katiraei, R. Iravani, N. Hatziargyriou, and A. Dimeas, "Microgrids management," *IEEE Power and Energy Magazine*, vol. 6, no. 3, pp. 54–65, May 2008, doi: 10.1109/MPE.2008.918702.
- [27] E. Espina, J. Llanos, C. Burgos-Mellado, R. Cárdenas-Dobson, M. Martínez-Gómez, and D. Sáez, "Distributed control strategies for microgrids: An overview," *IEEE Access*, vol. 8, pp. 193412–193448, 2020, doi: 10.1109/ACCESS.2020.3032378.

- [28] M. Saleh, Y. Esa, M. el Hariri, and A. Mohamed, "Impact of Information and Communication Technology Limitations on Microgrid Operation," *Energies* 2019, Vol. 12, Page 2926, vol. 12, no. 15, p. 2926, Jul. 2019, doi: 10.3390/EN12152926.
- [29] D. K. Molzahn *et al.*, "A Survey of Distributed Optimization and Control Algorithms for Electric Power Systems," *IEEE Trans Smart Grid*, vol. 8, no. 6, pp. 2941–2962, Nov. 2017, doi: 10.1109/TSG.2017.2720471.
- [30] "2018 - A Distributed Approach For OPF-Based Secondary Control of MTDC Systems | PDF | High Voltage Direct Current | Direct Current." <https://www.scribd.com/document/494637139/2018-A-Distributed-Approach-for-OPF-Based-Secondary-Control-of-MTDC-Systems> (accessed Jun. 20, 2022).
- [31] M. Yazdanian and A. Mehrizi-Sani, "Distributed control techniques in microgrids," *IEEE Trans Smart Grid*, vol. 5, no. 6, pp. 2901–2909, Nov. 2014, doi: 10.1109/TSG.2014.2337838.
- [32] Y. Wang, S. Wang, and L. Wu, "Distributed optimization approaches for emerging power systems operation: A review," *Electric Power Systems Research*, vol. 144, pp. 127–135, Mar. 2017, doi: 10.1016/J.EPSR.2016.11.025.
- [33] J. M. Guerrero, M. Chandorkar, T. L. Lee, and P. C. Loh, "Advanced control architectures for intelligent microgrids part i: Decentralized and hierarchical control," *IEEE Transactions on Industrial Electronics*, vol. 60, no. 4, pp. 1254–1262, 2013, doi: 10.1109/TIE.2012.2194969.
- [34] N. Prabakaran, A. R. A. Jerin, E. Najafi, and K. Palanisamy, "An overview of control techniques and technical challenge for inverters in micro grid," *Hybrid-renewable energy systems in microgrids: Integration, developments and control*, pp. 97–107, Jan. 2018, doi: 10.1016/B978-0-08-102493-5.00006-6.
- [35] M. H. Cintuglu, T. Youssef, and O. A. Mohammed, "Development and application of a real-time testbed for multiagent system interoperability: A case study on hierarchical microgrid control," *IEEE Trans Smart Grid*, vol. 9, no. 3, pp. 1759–1768, May 2018, doi: 10.1109/TSG.2016.2599265.
- [36] V. Nasirian, A. Davoudi, F. L. Lewis, and J. M. Guerrero, "Distributed adaptive droop control for DC distribution systems," *IEEE Transactions on Energy Conversion*, vol. 29, no. 4, pp. 944–956, 2014, doi: 10.1109/TEC.2014.2350458.
- [37] V. Nasirian, S. Moayedi, A. Davoudi, and F. L. Lewis, "Distributed cooperative control of dc microgrids," *IEEE Trans Power Electron*, vol. 30, no. 4, pp. 2288–2303, Apr. 2015, doi: 10.1109/TPEL.2014.2324579.
- [38] R. de Azevedo, "Fully Decentralized Multi-Agent System for Optimal Microgrid Control," 2016, doi: 10.25148/etd.FIDC000263.
- [39] C. Gavriluta, R. Caire, A. Gomez-Exposito, and N. Hadjsaid, "A Distributed Approach for OPF-Based Secondary Control of MTDC Systems," *IEEE Trans Smart Grid*, vol. 9, no. 4, pp. 2843–2851, Jul. 2018, doi: 10.1109/TSG.2016.2621775.
- [40] C. Godsil and G. Royle, "Algebraic Graph Theory," vol. 207, 2001, doi: 10.1007/978-1-4613-0163-9.
- [41] M. Mesbahi and M. Egerstedt, "Graph theoretic methods in multiagent networks," *Graph Theoretic Methods in Multiagent Networks*, Jul. 2010, doi: 10.1515/9781400835355.

- [42] A. Dorri, S. S. Kanhere, and R. Jurdak, "Multi-Agent Systems: A Survey," *IEEE Access*, vol. 6, pp. 28573–28593, Apr. 2018, doi: 10.1109/ACCESS.2018.2831228.
- [43] W. Ren and R. W. Beard, "Distributed Consensus in Multi-vehicle Cooperative Control," 2008, doi: 10.1007/978-1-84800-015-5.
- [44] F. Nejabatkhah and Y. W. Li, "Overview of Power Management Strategies of Hybrid AC/DC Microgrid," *IEEE Trans Power Electron*, vol. 30, no. 12, pp. 7072–7089, Dec. 2015, doi: 10.1109/TPEL.2014.2384999.
- [45] T. Dragicevic, X. Lu, J. C. Vasquez, and J. M. Guerrero, "DC Microgrids - Part I: A Review of Control Strategies and Stabilization Techniques," *IEEE Trans Power Electron*, vol. 31, no. 7, pp. 4876–4891, Jul. 2016, doi: 10.1109/TPEL.2015.2478859.